4-1984

The Effect of Air Knife Geometry on Coated Board Properties

Michael L. Iveson
Western Michigan University

THE EFFECT OF AIR KNIFE GEOMETRY
ON COATED BOARD PROPERTIES

by

Michael L. Iveson

A Thesis submitted
in partial fulfillment of
the course requirements for
The Bachelor of Science Degree

Western Michigan University
Kalamazoo, Michigan

April, 1984

ABSTRACT

The purpose of this thesis was to determine the effect of air knife angle and the distance between the air knife blades and backing-roll on coated board properties. Results of the experiment indicated that increasing the angle resulted in more uniform and smaller coated pores size. Increasing the distance resulted in more uniform pores with no effect on size. The optimum angle of operation was found to be between 17 and 20 degrees (approximate impingement angle) and optimum distance was determined to be between 80 and 90 mils. Further work that can be completed as a result of this thesis include; jet patterns of air knife isobars, locating exact optimization of angle and distance, determination of exact air jet angle, and the effect of orifice opening.

Keywords : Coaters; Air knife coaters; Geometry; Coated boards; Properties.

TABLE OF CONTENTS

LIST OF FIGURES

LIST OF FIGURES (cont.)

INTRODUCTION

The purpose of this thesis was to study the effect of air knife geometry on coated board properties. Air knife geomety was broken into three facets; the angle of the air knife, the distance between the air knife blades and the backing-roll, and the air pressure. The nozzle opening was kept constant.

The coated board was tested for physical and optical properties to determine the effect of air knife angle and distance on coated board properties. From the results of the data the most effective angle and distance for operation were found.

THEORETICAL DISCUSSION

Applications

With the development of the air knife, or air doctor coater at S.D. Warren in the 1930's, a new dimension of paper coating began. Since then however, blade coating techniques have caused an erosion in the grades once primarily air knife coated. This is due to the limitations in operating speeds, solids levels, and viscosities of air knife coatings.

These limitations have forced the air knife coater to be used in the following areas; paperboard coatings using clay and other organic pigments as a second or only coat; printing grades which require heavy, uniform thickness coatings for high quality; and specialty coatings including thermal, encapsulated, PVDC, and photographic coatings. (4)

These grades have remained air knife coated because they are in small markets and can command a high enough price to pay for the slower operating speeds. Due to this, little growth is foreseen in the use of the air knife coater. But even though the use is on the decline, future breakthroughs are a possibility, for this coating method is one of the most versatile, forgiving, and simple processes ever developed.

Types of Operation

The air doctor has three main types of operation; the brush type, the dam or metering type, and the true air doctor. These methods are displayed in figure 1. (1)

The first system, the brush type of operation, termed because the air doctor does only a small amount of metering. In this case, the

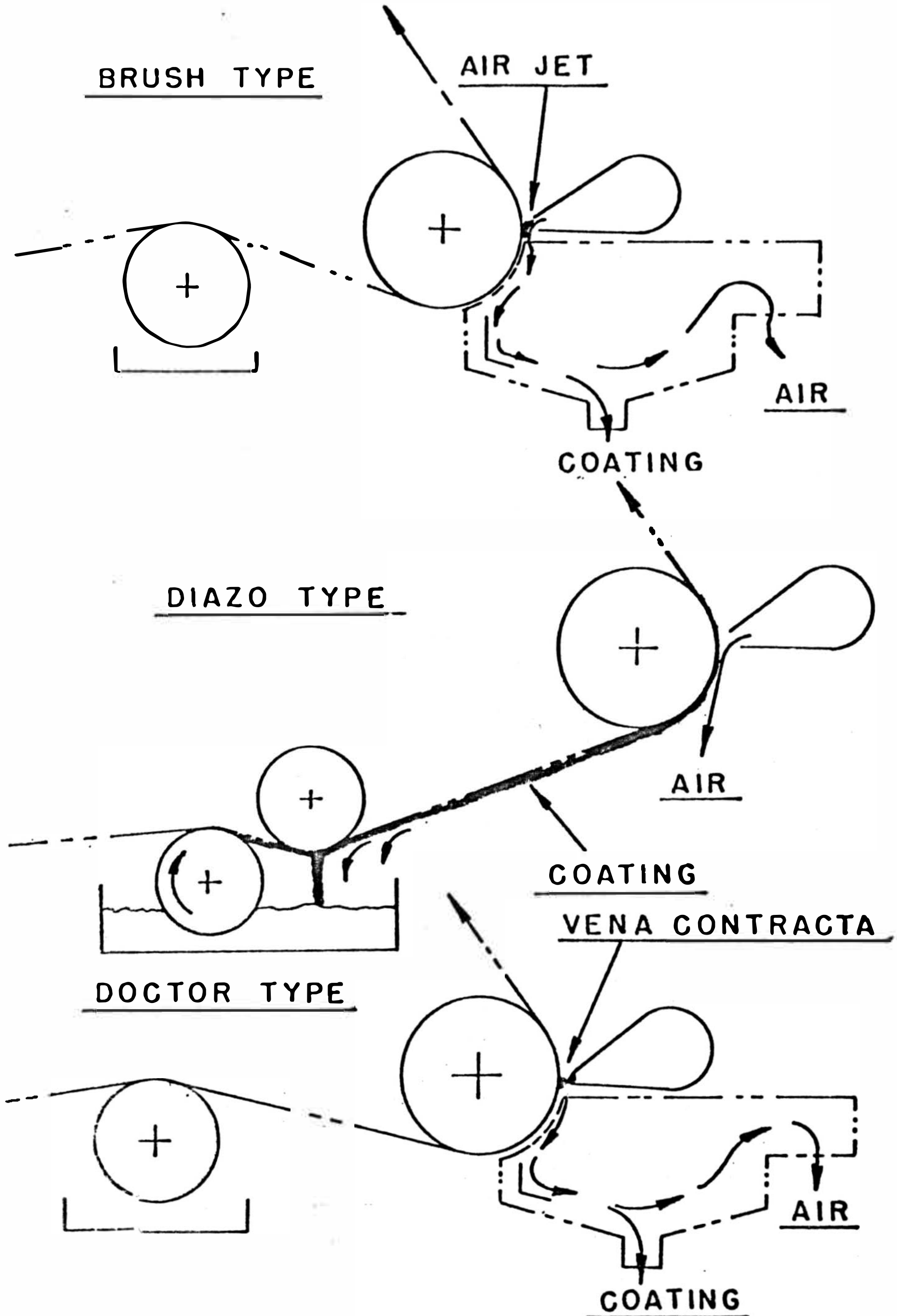

Figure 1. Three Types of Air Doctor Operation

jet of air issuing from the orifice acts more as a brush than as a metering doctor. This type of operation is necessary when the majority of the metering is completed at the application unit; the air brush is the final, minor, metering step. Due to the low pressures used, mottling of the coating can result very easily; thus to avoid this condition requires care.

Dam or metering type of operation is the second use of the air doctor. This system is primarily used in the diazo coating operation. In this case, the air doctor once again acts as a brush, but it also acts as a dam to prevent the excess coating from passing the air doctor. It blows the excessive coating from the sheet which drops off into the coating pan. This operation uses the air jet to do a certain amount of metering indirectly.

The last type of operation is the true air doctor. The true air doctor is dependent on the vena contracta of the jet to remove the excess coating. Using the sharpest edge of the air blast minimizes the problem of mottled, nonuniform coating and obtains the best control of metering.

Design

The air doctor itself is made up of two major parts - a large plenum chamber, and a set of blades. (see figure 2) The plenum accepts the air from the blower and delivers it to the blades, that form a nozzle for transforming air pressure to velocity.

There are several air knife designs on the market, however, the only major differences are found in the design of the blades. In almost all cases, one blade has a fixed position, while the other blade is mounted in such a way that it is adjusted relative to the fixed blade. The bottom blade is usually beveled or rounded on the inside of the chamber while

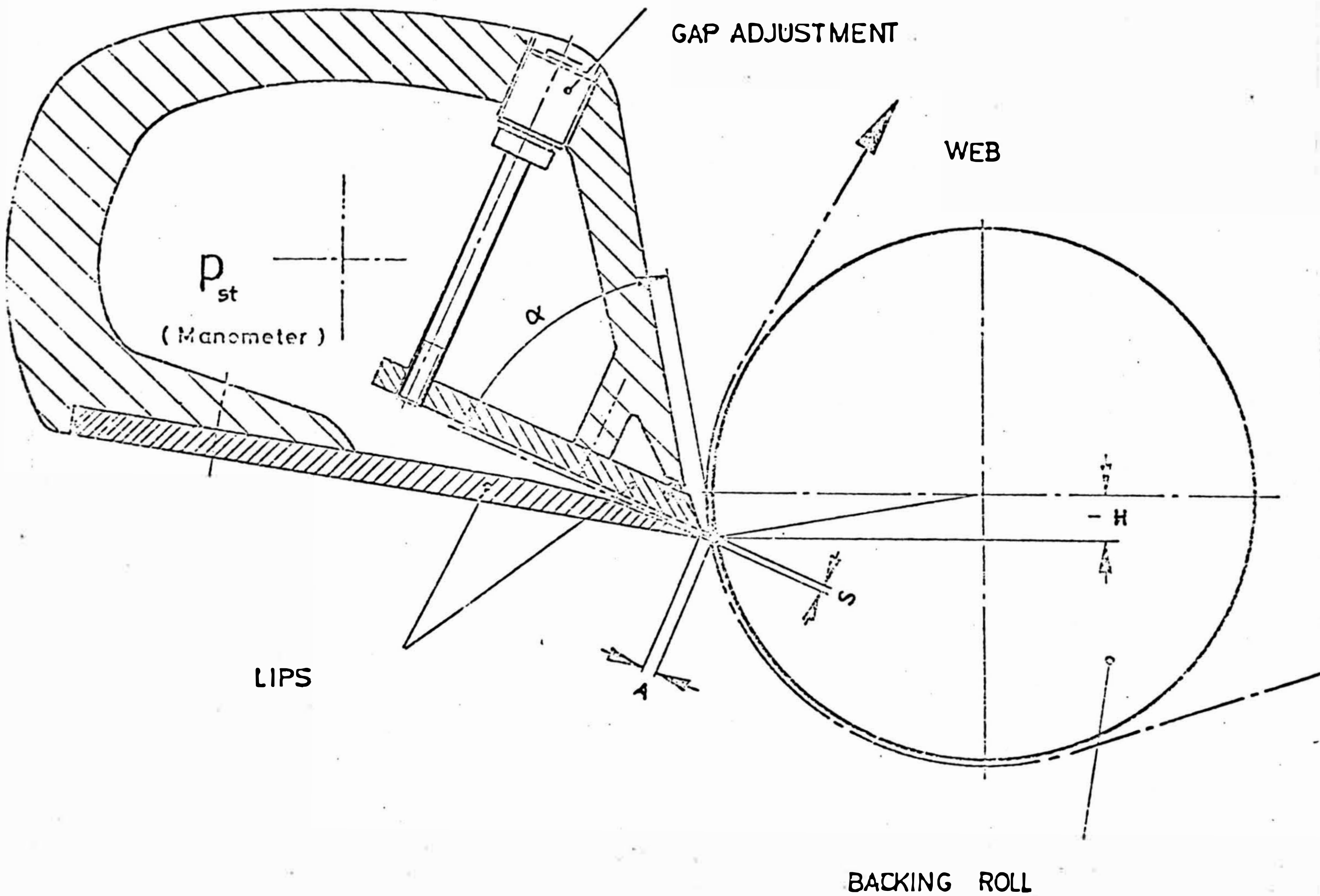

Figure 2

Air Knife/Backing-Roll Configuration

the top blade is beveled on the outside. This design allows the development of a converging air jet, and allows the sheet closer to the assembly. The converging blades allow the air jet to have maximum velocity where impingement on the coating occurs. During the original development of the blade configuration, it was found that the combination of one flat and one beveled blade gave the most efficient metering of coating with a minimum of coating mottle and coating spray. (1)

Static pressure in the plenum has a stronger influence on metering capacity than the adjustment of the orifice. Practical experience has confirmed theoretical calculations which show that slightly opening the gap between the blades increases the metering capacity. (5) The increase of the opening did not alter the internal static pressure in the plenum, but only increased the air volume.

The volume of air used in an air doctor varies with nozzle opening and pressure. The curve in figure 3 shows the air pressure - nozzle opening - volume ratio of a Warren-Dilts air doctor. This curve is quite similar for all air doctors, the only change is in efficiency of the nozzle in the conversion of pressure to velocity. Metering by an air doctor is a mass energy transfer; therefor, the velocity, volume, and temperature of the air are all important variables. (1)

It has been determined by Geza Kosta (3) that at an opening of 0.040 inches the air flow leaving the blade orifice is laminar. This laminar region extends approximately four times the distance from the end of the nozzle. This opening, however, is not the most efficient in practical operation. The most efficient opening is found by drawing a impact pressure vs. air pressure graph, at a distance away from the sheet. A certain opening gives a certain curve, drawing several curves determines the most efficient. The idea behind optimizing the nozzle opening is to

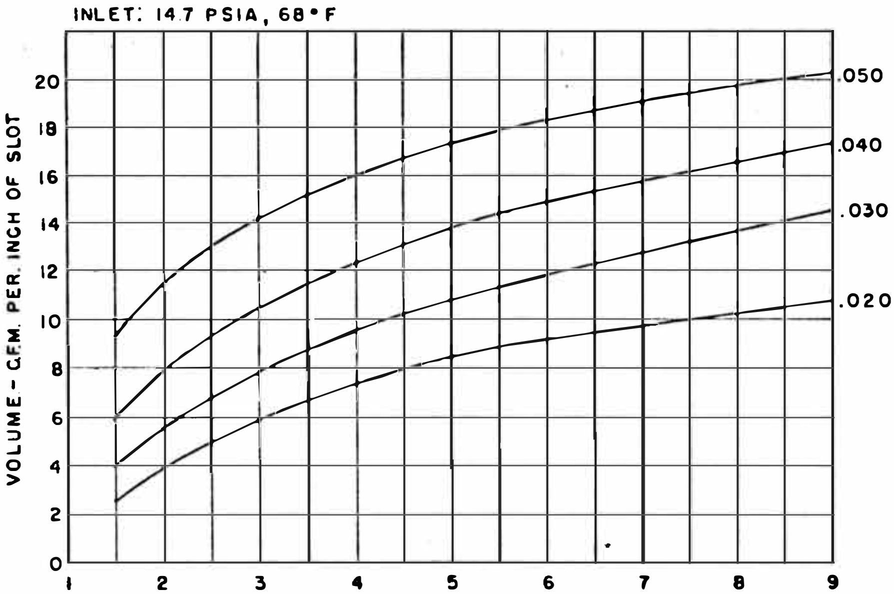

Figure 3. Air Pressure-Volume-Orifice Curves

maximize the metering effect and minimize the atomizing effect. The wider the nozzle opening the greater the effect of atomizing. This follows for a much greater volume of air is used; it is working over a wider area, and the atomizing of more coating will occur.

The optimum orifice opening of 0.040 inches is used to display the effect of pressure. The jet produced will be at the highest velocity at which a laminar flow is projected the farthest from the orifice into the open atmosphere. Beyond the jet there is a cone of turbulence. If the pressure is raised, the cone of turbulence tends to move closer to the orifice, thus shortening the jet. Increasing the pressure further increases the impact pressure that is produced; however, if the pressure is raised, the cone of turbulence moves closer to the orifice, more eddies are formed, and more energy is dissipated in turbulent mixing. Coating is readily atomized in the turbulent mixing area. (5)

Kosta (3) also determined that many nozzles produced approximately the same general pattern of isobars, so far as the length and the shape of the jet are concerned. This can be seen in figure 4. The pressure cone does most of the metering; therefor, the optimum impact area is somewhere less than 3/8 inch from the orifice. Positioning of the air knife too close to the coating produces fouling of the blades, splitting the air stream, and coating streaks. If the air knife is too far away from the backing-roll, brushing takes place. Also, to a greater extent, the distance from the blades to the backing-roll is dependent on the condition of the blades.

In coater design, the positioning of the air knife is often above or below the backing-roll horizontal centerline. This is to prevent web flap, which causes coating patterns. This must be taken into account when the angle of the air knife is determined. If the air knife is not

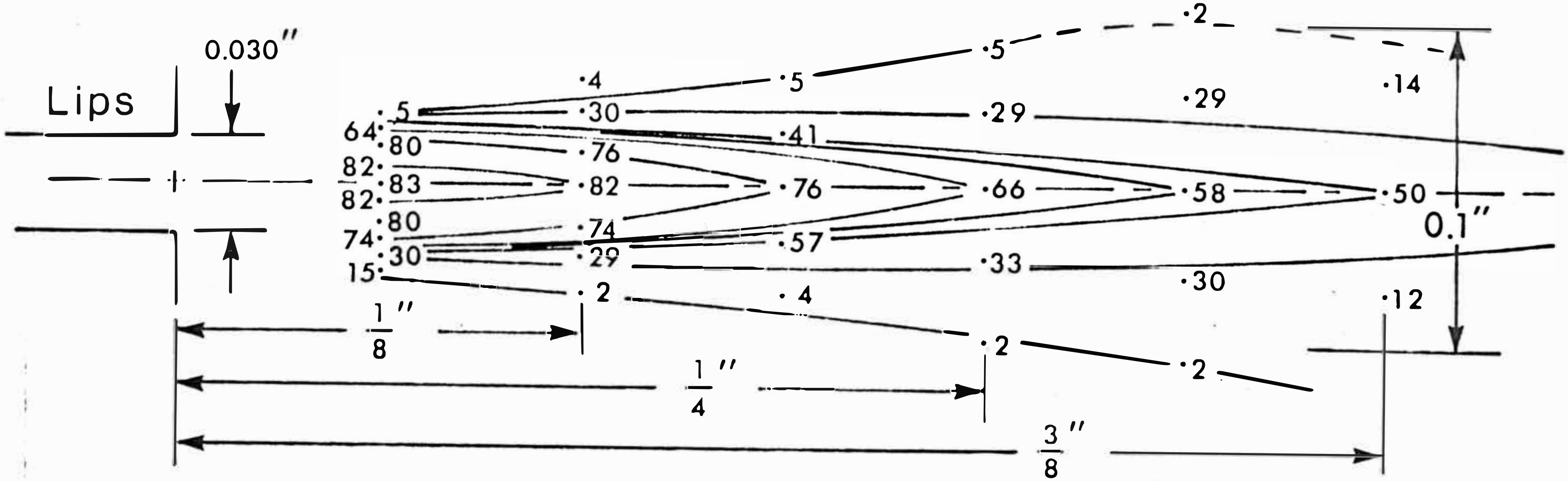

Figure 4. Typical Jet Pattern
(20x actual size)

properly positioned, with respect to the offset from the backing-roll centerline and the angle, there isn't enough room for the expanding air to escape. The failure to leave enough room for this air to escape will tend to foul the nozzle. Through years of experience, Kosta (3) determined that there is no reason to raise or lower the air knife for different grades. This only aggravates the problem of spraying and misting. Simply setting the air knife a fixed distance from the backing-roll centerline for multi-purpose use will surfice.

The angle at which the air knife is positioned influences the metering capacity. The jet of air impinges the coating, dividing it. At an angle there will always be a component that goes back against the direction of the original flow. In reversing itself, it picks up all the air entrained coating and deposits it on the top of the air knife. The deposit usually creates a problem with streaks in the coating; therefor, a compromise in this instance is essential. This is made up of a combination of air knife angle and distance from the backing-roll,allowing the escaping air from the reversing component to release. (3)

The Warren coater, used in experimentation, has asymmetrical blades in that the top blade has parallel surfaces with a champfered tip and the bottom blade has a radius on the internal surface. The result is that the air exits the orifice in a downward fasion at an angle of 8 degrees from the inner surface of the top blade. (6) Therefor, any measurement taken in experimentation must include 8 degrees to attain the correct impingement angle of the air jet.

Base Stock Condition

Suursalmi (2) showed that at speeds over 150 m/min, stock absorbency had a negligible effect on coat weight. He noticed that coat weight differences always are derived from base paper roughness, higher roughness always results in higher coat weights. Figure 5 is a graph which illustrates coat weight vs. machine speed. At lower machine speeds, filter cake formation causes a decrease in coat weight, due to the increase in dwell time between application and metering.

Filter Cake Theory

The filter cake theory mentioned above is an important concept in the operation of an air knife coater. This theory states that the water and some of the soluble penetrates into the paper leaving the coating. As this penetration is taking place, the coating at the paper-coating interface becomes higher in solids, while the coating at the surface is relatively unaffected. When the sheet passes under the air doctor jet, the top, less viscous layer is removed, shearing at the point where the filter cake begins. This zone, where the shearing takes place, is the transition area from the fluid to semi-plastic coating. (1) The exact point at which this shearing takes place is dependent on the amount of energy imparted on the sheet. (see figure 6) This theory also explains the dependence of viscosity and solids level in the coating and how it affects the coat weight. It also points toward the reasoning behind calling the air knife a contour coater.

The air knife is considered a contour coater because the coating remaining has uniform thickness over the surface of the sheet. Since the surface of the sheet is quite rough, with fibers in a variety of positions on the surface of the sheet, the coating will tend to follow that surface. The uniformity of the coating layer is dependent on the filter cake theory. If the water penetrates uniformly over the entire surface of the sheet, it will produce a uniform filter cake. Since the air knife simply removes the less viscous coating, a uniform layer of higher viscosity coating is left. (4)

Solids

As mentioned above, viscosity and solids level are limiting factors in the operation of an air knife coater. Solids level is perhaps the more important of the two due to the fact that if the solids level is too high, the filter cake will develope too rapidly, and result in higher than desired coat weights. In this case, the air knife is unable to remove the excess coating and air pressure cannot control it, which is the primary means of coat weight control. Another influence on the level of solids is the absorbability of the paper, less absorptive paper will allow higher solids coating, while highly absorptive paper will need lower solids. (4)

Viscosity

The effect of viscosity of the coating is seen throughout the operation of the air knife. The main theory relating the effect of viscosity states that the higher the viscosity of the coating, the more it will resist the scraping effect of the air knife. This tends toward higher coat weights, and in practical operation this is proven. High viscosities cause other problems as well. Coat weight variations are seen if the coating leaving the applicator system is not level. It can also cause "stipple", the splitting of the coating layer between the paper and the applicator roll causing a roughened surface. Lastly, high viscosities cause problems in the catch pan and return systems, since these operations usually depend on gravitational flow. (4)

However, if the viscosity becomes too low, the coating will run off, or begin to run off, before reaching the air knife. This causes a non-uniform thickness introduced to the air knife, leading to a non-uniform coating leaving the air knife. Since the air knife has only a certain amount of energy available for coating removal, and if that energy is expanded before the necessary amount of coating is removed, a high coat weight will result. (4)

Application of Coating

The application of coating is fairly important in the control of coat weight. Although there are several types of applicator systems, this paper will only discuss the single-roll or kiss-roll applicator, since it is the system on the pilot coater used in the experimental work. Suursalmi (13) found that at low machine speeds there was no change in coat weight as the applicator roll speed increases, the applied layer becomes thicker, as shown in figure 7. However, at low machine speeds the air knife can remove all excess coating. As machine speed increases, the amount applied begins to effect the coat weight. This relates back to the filter cake theory and the time involved for the coating to penetrate into the sheet. As the speed increases further it becomes harder to control coat weight effectively, this is seen in figure 8.

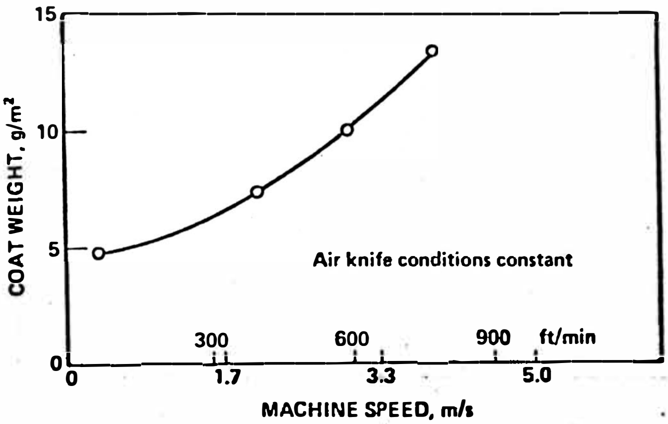

Figure 5. Coat Weight vs. Machine Speed. (substrate has high absorbency)

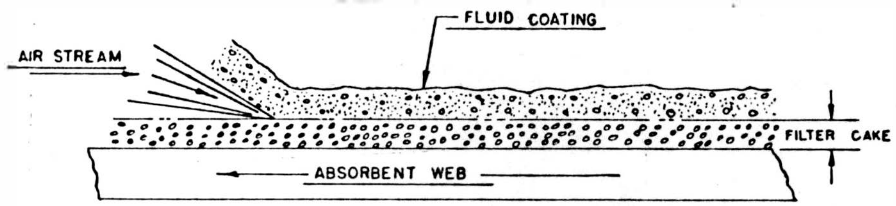

Figure 6. Filter Cake Theory of Air Doctor Coating

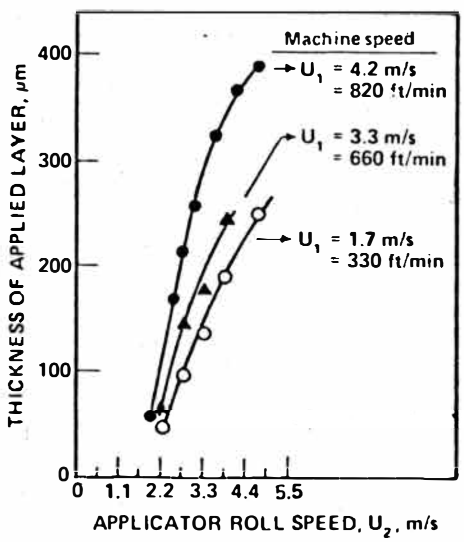

Figure 7. Applied Coating Layer Thickness vs. Applicator Roll Speed

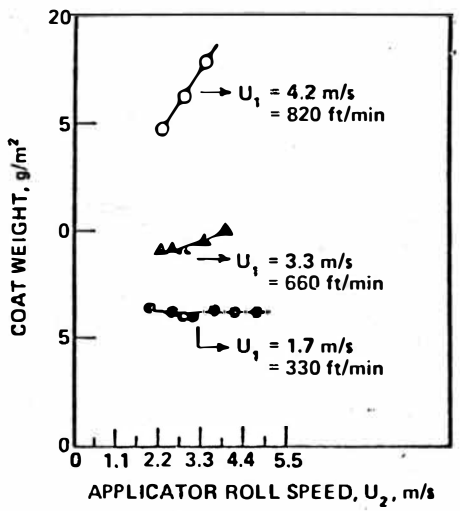

Figure 8. Coat Weight vs. Applicator Roll Speed

EXPERIMENTAL PROCEDURE

Materials

Paperboard used in this thesis was donated by James River Corp., Brown Paper Div., Kalamazoo, Michigan. The rolls were aquired and slit down to 22½ inch widths for use on the pilot coater. The board caliper was 17.5 point, with variations of approximately ± 1 point.

The materials used in the coating were; Engelhard HT predispersed #2 clay, Anatase LW TiO_2, Hercules L7 CMC, Dow 620 SBR latex, and Dispex dispersing agent.

Equipment

Coating preparation was completed with floor and tank cowles located at the rear of the coater. The machine run was completed on the WMU pilot coater using the Warren-Dilts air knife, serial no. 361 60, model no. 31. Testing equipment, with the exception of the gloss meter, was obtained from WMU. They include; Parker Print Surface, brightness meter, K&N ink, Sheffield smoothness, IGT pick tester, and the analytical scale. The use of the gloss meter was donated by Hercules.

Procedure

Coating Preparation

Coating preparation began with the dispersion of 1.4 lb. of CMC in 28 lb. of water, obtaining a 0.2% solution by volume. The CMC was predispersed in enough isopropyl alchol to make a paste, then stirred into the water slowly for two hours. After the solution was well mixed, it was sifted with a 40 mesh screen to remove clumps and foreign particles.

Titanium dioxide was dispersed at 75% solids in the floor cowles for 20 minutes. This mixture included 30 lb. TiO_2, with 10 lb. of water. The slurry was tested by feel to make sure all particles were in solution.

Water, 116 lb., was placed in the tank cowles and the motor was set to the third position, dispex was added at 0.15%, then clay was added slowly until the total 270 lb. was combined with the water. This resulted in a 70% solids solution. The cowles speed was increased to five for 30 minutes.

After this time period the TiO_2 was added and allowed to mix for another 15 minutes. Following this, the remainder of the water was added, 97.3 lb., reducing the solids level to 57.3%. The cowle was drained into buckets and placed in a paperboard drum for aging.

When the coating cooled, the addition of latex began. Dow 620 latex was added a little at a time, stirring 73.4 lb. in with a broom stick. After complete mixture of the latex, addition of CMC took place in the same manner. It should be noted that continual solids and viscosities were taken at each step of addition to make sure the coating was at the correct level. The resulting coating recorded at 53.6% solids and 240 centipoise (100 RPM, #4 spindle).

The following figure illustrates the coating formulation used.

Figure 9
Coating Formulation

#2 Clay	90 parts/100
TiO_2	10 parts/100
SBR	12 parts/100
CMC	0.2% by volume

The complete mixing formulation is documented in Appendix A.

Machine Run

Prior to the machine run, the statistics department was consulted to develope an experimental design. A grid was set up to cover the angles and distances required. This can be seen in Appendix B. The following table shows the run number and the corresponding angle and distance.

Table 1

Machine Run Numbers
Corresponding Angle & Distance

Machine Run	Angle	Distance
1	3	50
2	3	80
3	3	110
4	6	70
5	6	90
6	6	120
7	9	60
8	9	100
9	9	130
10	12	50
11	12	70
12	12	90
13	12	120
14	15	60
15	15	80
16	15	100
17	15	130
18	18	50
19	18	90
20	18	110

The machine run was completed with the following constant variables; machine speed (250 ft/min), dryer stage temperatures (125°F/135°F/145°F), nozzle opening (0.020 in.), and applicator speed. The machine variables were air knife angle, distance between air knife blades and backing-roll, and air pressure.

Air knife angle was changed after the completion of each distance at that angle. The angle was measured with a construction angle indicator, and changed with the adjustment bolts on the machine. As seen in the grid, the angles ranged from 3 to 18 degrees at 3 degree intervals. Adjustment of the distance was measured with a feeler gauge, measured in thousand's of an inch. The distance ranged from 50 to 130 mils, in 10 mil intervals. The air pressure was measured with the dial attached to the outlet pipe of the air pump. Moving the plate over the outlet pipe adjusted the air pressure from 1, 2, and 3 psi.

After the machine run, final viscosities and solids were taken to determine the state of the coating as it was used. The viscosity was run at 100 RPM with a #4 spindle, on four samples, and averaged 240 centipoise. The solids level was completed by taking four samples and determining the water content before and after drying 24 hours, they averaged 53.6%.

Testing

Rolls resulting from the machine run were slabbed down, and samples were taken from the resulting sheets. The sheets were sampled to attain ten six inch disks, and five one inch strips for testing. These samples were labeled and conditioned in the student testing lab for three days.

Testing began with determining the coat weights on the analytical balance. During the machine run $8\frac{1}{2}$ x 11 sheets were attached to the web prior to coating application and metering, after finding these areas, disks were cut from them and were used as the base sheet comparison for that section of the run. The difference in coated and non-coated disks were converted to coat weight in lb/24 x 36 ream.

Tests discussed in this paragraph all involved taking ten readings, one on each coated disk. Gloss and brightness readings were taken in the machine direction, prior to the contact tests. Sheffield smoothness was recorded. Then Parker Print Surface was recorded at the 10 and 20 kg/m^2 values. Following these tests K&N ink was completed (brightness difference after two minutes of ink contact), and C-stain (brightness difference after five seconds of stain contact; note; uniform stain layer was obtained by placing four drops on a microscope slide, and placed on the sheet for five seconds).

IGT picks were completed with the use of five one inch strips, the pick tester was set at 1.5 cm/sec accelerating speed, and applying number 5 tack ink.

RESULTS PRESENTATION

Tables of the oomplete data set are reoorded in Appendix C. The tables on the effect of angle are found in Appendix D, and the tables on the effect of distance are found in Appendix E.

Appendix F includes the graphs of angle, and distance, versus the coated board properties. At each angle and distance, each test was plotted against coat weight, drawing the best straight line through the three pressures used. From these plots a common coat weight was chosen, 10 lb/24 x 36 ream, and the corresponding test values were recorded on the graph of angle or distance.

DISCUSSION OF RESULTS

The discussion will begin with the results of the coating tests versus air knife angle. Figure 10 displays brightness versus angle, showing an upward trend from 67% to 71%. Brightness is a measure of percent reflectance, measuring the uniformity of air filled pores, thus as angle increases the pore structure becomes more uniform.

Figure 11 displays gloss versus air knife angle. The gloss reading ranged from 29% to 35%, however, the strange configuration is probably explained by the difference in the two rolls, which were changed between 9 and 12 degrees. Each case does show a decreasing gloss with increasing angle. Gloss is a measure of pore volume size, the higher the gloss the higher the higher the pore volume size, thus as angle increases the pore volume decreases.

Figure 12 shows Sheffield smoothness versus air knife angle. A drastic decrease in smoothness is seen as angle increases, ranging from 134 to 113 Sheffield units. This relates back to the more uniform pore structure, and decreasing pore volume, resulting in a smoother coated board.

Figures 13 and 14 display Parker Print Surface versus air knife angle. Parker Print Surface measures the variation of coating depth in microns. The results show little change with increasing angle, however, a slight decrease in depth was noticed at higher angles. The readings ranged from 4.17 to 3.95 microns, this is not suprising because the air knife is known as a contour coater.

Figure 15 shows K&N ink versus air knife angle. As the angle increases, K&N ink hold out decreased. This demonstrates that less ink was absorbed due to the decrease in pore size. The values ranged from 17.6% to 11.6%.

Figure 16 illustrates the effect of C-stain on the coating as the air knife angle increased. This test shows the same trend as gloss in that the results were effected by the changing of the rolls. This treatment was chosen to determine how the coating would be effected by a different type of solvent than ink for receptivity, however, the result of angle displayed little. The values ranged from 14.1% to 12.4%.

The last figure, 17, displays IGT picking strength versus air knife angle. The values ranged from 78.2 cm to 60.4 cm, increasing as the angle increased, leveling from 12 to 18 degrees. It is noted that maximum film strength occurs with a well orientated coating film; therefor, orientation increases with increased angle, and relating to a more uniform pore size.

The remainder of the discussion will deal with the coating tests versus the distance between the air knife blades and the backing-roll. Brightness versus distance is displayed in figure 18. The brightness readings ranged from 66.6% to 69.8%, increasing as distance increased. This shows that the air filled pores become more uniform as distance increased.

Figure 19 illustrates gloss versus distance, and as mentioned before, gloss is related to poor volume. The results of this graph show relatively little, as the values range from 34.0% to 31.5%, and have little trend, leaning toward a slight increase.

Figure 20 shows Sheffield smoothness versus distance. The Sheffield smoothness values range from 118 to 132 Sheffield units, but shows no trend as distance increases.

Figures 21 and 22 display Parker Print Surface versus distance. The values for Parker Print Surface at 10 kg/m^2 range from 4.0 to 4.08 microns, while 20 kg/m^2 values range from 3.03 to 3.09 microns. But show flat trends in surface depth as distance increases. Once again showing why the air knife is considered a contour coater.

K&N ink receptivity versus distance is shown in figure 23. K&N ink receptivity is effected by coating pore structure. The values resulting from this experiment ranged from 15.4% to 13.4%, and showed a constant trend. Thus, K&N ink recepivity was not effected by distance.

Figure 24 shows the effect of C-stain versus distance. The C-stain values ranged from 14.6% to 12.4%. The graph displays a upward trend to 80 mils, then decreases as distance increases. This shows that this particular penetrant is effected by distance to a point where the pore structure decreases and penetration becomes more difficult.

The last figure, 25, displays IGT picking strength versus distance. The pick values range from 60.5 to 80.5 cm, arranged in an increasing pattern as distance increased. This indicates that the orientating film increases the picking strength as distance increases.

CONCLUSIONS

The conclusions drawn from the results are as follows:

1. As air knife angle increases, a more uniform pore structure evolves.

2. As air knife angle increases, pore volume size decreases.

3. As the distance between the air knife blades and backing-roll increases, a more uniform pore structure evolves.

4. As distance increases, it has no effect on pore volume size.

5. The optimum air knife angle for operation is between 9 and 12 degrees. (as measured from the machine)

6. The optimum distance between the air knife blades and the backing-roll is between 80 and 90 mils.

RECOMMENDATIONS

Further work that can be undertaken as a result of this thesis includes; jet patterns of air knife isobars, locating closer angle and distance measurements for optimization, determination of exact angle of the air jet, and effect of orifice opening.

1. Efficiency can be increased by drawing an impact pressure versus air pressure graph; therefor, maximizing the metering effect and minimizing the atomizing effect. A graph of this nature will display the isobars of the air knife, showing the pressure cone (used for metering), and the cone of turbulence (causing atomizing).

2. Further investigation in the same manner as this thesis might show a closer point of optimization for air knife angle and distance between the air knife blades and backing-roll, narrowing the gap between 9 and 12 degrees and 80 to 90 mils.

3. From photographs and a strobe light the calculation of the exact air knife angle could be calculated. This information would be helpful in combination with the first recommendation to determine what the air jet is actually doing.

4. A study could be completed to determine the effect of the orifice opening on the operation of the air knife, and how this effects the pressure and turbulent cones.

A combination of the completion of these recommendations will result in a full understanding of the operation and optimization of the WMU pilot air knife coater.

LITERATURE CITED

1. Booth, G.L., "Coating Equipment and Processes" New York Lockwood Publ. Co., 1970, Ch. 10, p. 92

2. Suursalmi, J., TAPPI 66 (5): 81 (1983)

3. Kosta, G.L., Janett, G., and Alexander, D.R., "Air knife Theory and Practice" Midland-Ross Air Knife Seminar, April 1978

4. Kline, J., TAPPI Ch. 9 Home Study Course

5. Booth, G.L., "Equipment Aspects of PVDC Coating" paper given to WMU 8th Annual Specialty Coating and Laminations Seminar, August 1978

6. Booth, G.L., "The Air Knife Coater Past and Present" TAPPI Air Knife Coating Seminar, Atlanta, Nov. 1981

7. Black Clawson Air Doctor Coater Manual

8. Frost, F.H., TAPPI 40 (8): 152A (1957)

9. Kallock, W.F., Paper Trade J. :32 (April 1, 1957)

10. Bohmer, E., Svensk Papperstidning :673 (Oct. 31, 1967)

11. Willets, W.R., TAPPI 33 (4): 201 (1950)

12. Suursalmi, J., "Limiting Factors in Air Knife Coating", paper given to TAPPI Coating Conference, 1982

APPENDIX A

Complete Mixing Formulation

270 lb. #2 Clay @ 70% solids 386 lb. total	116 lb. water
30 lb. TiO_2 @ 75% solids 40 lb. total	10 lb. water
1.4 lb. CMC (0.2% of volume) @ 5% solids 28 lb. total	26.6 lb. water
36 lb. SBR @ 49% solids 73.5 lb. total	37.5 lb. water
337.4 lb. dry total	190.1 lb. water total

$\frac{337.4}{0.54}$ = 624.8 - (337.4 + 190.1) = 97.3 lb. water to add

APPENDIX B

Angle and Distance Grid

Distance (mils)

	50	60	70	80	90	100	110	120	130
3	1			2			3		
6			4		5			6	
9		7				8			9
12	10		11		12			13	
15		14		15		16			17
18	18				19		20		

APPENDIX C

TABLE II

Complete Data Set

angle/distance pressures

Coat Weight (lb/ream)

angle/distance	1	2	3
3/50	11.33	7.17	6.50
3/80	12.41	6.76	5.15
3/110	12.83	10.09	8.12
6/70	13.29	11.20	13.29
6/90	14.03	10.12	7.78
6/120	17.01	9.83	8.94
9/60	12.76	9.14	6.54
9/100	15.92	7.01	8.08
9/130	15.27	9.69	6.20
12/50	11.55	6.24	7.03
12/70	12.33	7.25	5.05
12/90	12.42	7.94	6.57
12/120	20.00	10.38	7.29
15/60	13.67	10.69	8.05
15/80	13.15	10.28	9.08
15/100	20.95	14.24	10.45
15/130	20.54	18.55	13.40
18/50	18.94	10.04	7.71
18/90	23.78	15.60	11.30
18/110	26.98	17.93	13.47

angle/distance	Brightness (%)			K&N ink (%)		
3/50	71.07	64.89	61.63	14.29	17.15	21.16
3/80	71.42	65.69	62.50	11.70	15.28	17.74
3/110	73.22	67.24	63.78	11.51	14.66	18.19
6/70	71.65	65.60	71.65	12.93	18.01	12.93
6/90	72.38	67.00	63.86	12.95	17.64	20.89
6/120	74.13	68.83	65.67	12.00	15.61	19.03
9/60	72.09	66.29	62.66	12.61	17.43	20.20
9/100	73.58	68.48	65.00	12.41	18.67	21.29
9/130	75.45	70.52	67.22	11.00	15.13	19.17
12/50	71.79	66.69	63.13	13.43	17.95	19.98
12/70	72.36	66.53	62.68	11.47	15.97	17.59
12/90	73.11	67.43	64.31	10.77	14.51	17.28
12/120	77.27	71.95	67.03	9.08	11.48	13.33
15/60	71.86	65.94	62.83	11.49	14.85	17.16
15/80	72.45	68.91	65.75	11.06	12.27	15.82
15/100	77.76	73.29	69.84	8.56	10.87	13.69
15/130	76.69	75.50	72.36	7.48	9.59	11.62
18/50	76.76	72.40	68.51	9.68	11.72	13.77
18/90	78.82	75.45	71.63	8.68	9.15	10.62
18/110	78.79	76.25	72.83	7.99	9.54	10.69

APPENDIX C

TABLE II (cont.)

angle/distance	C-stain (%) pressures 1	2	3	Gloss (%) 1	2	3
3/50	13.4	13.8	13.2	31.5	29.5	25.4
3/80	14.5	14.2	14.5	32.5	30.2	29.3
3/110	13.6	14.0	14.6	33.4	30.5	29.7
6/70	11.1	12.4	13.5	31.1	29.5	31.1
6/90	11.9	12.8	13.4	33.1	29.8	29.9
6/120	12.5	11.4	13.1	31.6	29.1	29.1
9/60	12.2	13.1	15.6	30.2	28.9	28.1
9/100	10.2	11.7	14.1	30.8	27.4	27.4
9/130	10.1	11.9	12.9	32.0	29.1	27.6
12/50	11.8	12.2	12.3	30.9	27.2	28.8
12/70	15.3	14.7	17.5	40.4	36.9	35.0
12/90	13.8	15.6	13.6	36.9	35.5	34.6
12/120	13.2	12.9	16.7	42.5	34.8	33.7
15/60	12.9	14.4	13.6	36.4	35.6	33.1
15/80	13.4	16.1	14.0	37.4	32.7	33.3
15/100	15.1	14.1	13.2	41.6	36.8	34.7
15/130	12.5	12.4	11.5	47.6	43.2	39.9
18/50	14.9	13.4	14.1	39.8	34.3	34.5
18/90	11.8	12.8	14.8	46.8	38.4	35.3
18/110	10.8	12.0	13.0	44.5	37.8	35.2

angle/distance	Sheffield Smoothness 1	2	3	IGT pick 1	2	3
3/50	135	133	130	69.6	83.6	88.8
3/80	147	122	123	54.2	65.4	86.8
3/110	137	121	136	61.8	57.4	74.8
6/70	135	133	135	34.8	49.0	34.8
6/90	127	136	123	64.8	75.2	40.6
6/120	151	141	126	72.0	56.0	66.6
9/60	146	139	136	68.8	70.6	65.4
9/100	162	151	140	81.6	81.8	88.4
9/130	179	163	150	77.0	82.2	67.4
12/50	118	116	107	71.8	69.6	78.2
12/70	95	107	100	72.4	78.4	89.0
12/90	124	115	110	73.8	83.8	97.8
12/120	139	116	109	82.4	87.8	92.0
15/60	122	111	115	71.2	71.8	70.6
15/80	131	122	120	62.8	69.4	70.8
15/100	135	119	112	61.0	78.2	81.0
15/130	119	112	108	65.2	67.4	82.6
18/50	141	121	118	74.6	70.6	77.6
18/90	128	118	119	56.6	84.8	73.8
18/110	154	145	141	84.4	79.2	70.0

APPENDIX C

TABLE II (cont.)

angle/distance	pressures Parker Print Surf. 10 kg/m^2 1	2	3	Parker Print Surf. 20 kg/m^2 1	2	3
3/50	4.15	4.23	4.38	3.09	3.18	3.35
3/80	4.28	4.10	4.31	3.19	3.08	3.23
3/110	4.15	4.06	4.11	3.11	3.08	3.06
6/70	4.18	4.08	4.18	3.15	3.11	3.16
6/90	4.12	3.97	4.05	3.14	3.07	3.07
6/120	4.31	4.20	4.15	3.23	3.15	3.08
9/60	4.16	4.27	4.40	3.08	3.21	3.36
9/100	4.38	4.32	4.24	3.31	3.26	3.18
9/130	4.59	4.36	4.36	3.48	3.31	3.33
12/50	3.97	4.06	3.95	3.00	3.11	3.02
12/70	3.68	3.86	3.98	2.84	3.03	3.06
12/90	3.99	3.99	4.07	3.06	3.04	3.14
12/120	4.04	3.90	3.89	3.14	3.01	3.02
15/60	3.90	3.96	4.07	3.03	3.05	3.13
15/80	4.08	4.21	4.04	3.15	3.23	3.13
15/100	4.10	4.03	3.98	3.17	3.11	3.07
15/130	3.68	3.61	3.69	2.85	2.82	2.86
18/50	4.06	4.11	3.96	3.17	3.18	3.10
18/90	3.97	3.87	4.00	3.10	2.96	3.09
18/110	4.21	4.13	4.10	3.29	3.14	3.12

APPENDIX D
TABLE III

Angle Data Set

Coat Weight (lb/ream)

angle	pressures 1	2	3
3	12.19	8.01	6.59
6	14.78	10.38	10.00
9	14.65	8.61	6.93
12	14.08	7.95	6.49
15	17.08	13.44	10.25
18	23.23	14.52	10.83

Brightness (%)

angle	1	2	3
3	71.90	65.94	62.64
6	72.72	67.14	67.06
9	73.71	68.43	64.96
12	73.63	68.15	64.29
15	74.69	70.91	67.70
18	78.12	74.70	70.99

K&N ink (%)

angle	1	2	3
3	12.50	15.70	19.03
6	12.63	17.09	17.62
9	12.01	17.08	20.22
12	11.19	14.98	17.04
15	9.65	11.90	14.57
18	8.78	10.13	11.69

C-stain (%)

angle	1	2	3
3	13.85	14.03	14.03
6	11.82	12.17	13.27
9	10.83	12.25	14.21
12	13.56	13.84	15.08
15	13.44	14.39	13.11
18	12.55	12.72	13.95

Gloss (%)

angle	1	2	3
3	32.5	30.1	28.1
6	31.9	29.5	30.0
9	31.0	28.5	27.7
12	37.7	33.5	33.0
15	40.8	37.1	35.3
18	43.7	36.8	35.0

Sheffield Smoothness

angle	1	2	3
3	139	125	130
6	138	137	128
9	162	151	142
12	119	114	106
15	127	116	114
18	141	128	126

IGT pick (cm)

angle	1	2	3
3	61.9	68.8	83.5
6	57.2	60.1	47.3
9	75.8	78.2	73.7
12	75.1	79.9	89.3
15	65.1	71.7	76.3
18	71.9	78.2	73.8

Parker Print Surf. 10 kg/m^2

angle	1	2	3
3	4.19	4.13	4.27
6	4.20	4.08	4.13
9	4.38	4.32	4.33
12	3.92	3.95	3.97
15	3.94	3.95	3.94
18	4.08	4.04	4.02

Parker Print Surf. 20 kg/m^2

angle	1	2	3
3	3.13	3.11	3.21
6	3.17	3.11	3.10
9	3.29	3.26	3.29
12	3.01	3.05	3.06
15	3.05	3.05	3.05
18	3.19	3.09	3.10

APPENDIX E

TABLE IV

Distance Data Set

Coat Weight (lb/ream)

distance	pressure 1	2	3
50	13.94	7.82	7.08
60	13.21	9.91	7.29
70	12.81	9.22	9.17
80	12.78	8.52	7.11
90	16.75	11.22	8.55
100	18.43	10.62	9.24
110	19.91	14.01	10.80
120	18.50	10.10	8.12
130	17.91	14.12	9.80

Brightness (%) / K&N ink (%)

distance	Brightness 1	Brightness 2	Brightness 3	K&N ink 1	K&N ink 2	K&N ink 3
50	73.20	67.99	64.42	12.47	15.61	18.30
60	71.98	66.12	62.75	12.05	16.14	18.68
70	72.01	66.06	67.17	12.20	16.99	15.26
80	71.94	67.30	64.13	11.38	13.78	16.78
90	74.77	69.96	66.60	10.80	13.77	16.26
100	75.67	70.89	67.42	10.49	14.77	17.49
110	76.01	71.75	68.31	9.75	12.10	14.44
120	75.70	70.39	66.35	10.54	13.55	16.18
130	76.07	73.01	69.79	9.24	12.36	15.40

C-stain (%) / Gloss (%)

distance	C-stain 1	C-stain 2	C-stain 3	Gloss 1	Gloss 2	Gloss 3
50	13.43	13.13	13.18	34.1	30.3	29.6
60	12.60	13.80	14.60	33.3	32.3	30.6
70	13.25	13.43	15.43	35.8	33.2	33.1
80	13.80	15.40	14.20	35.0	31.5	31.3
90	12.50	13.77	13.90	38.9	34.5	33.3
100	12.65	12.90	13.63	36.2	32.1	31.1
110	12.33	13.00	13.80	39.0	34.2	32.5
120	12.80	12.15	15.00	37.1	32.0	31.4
130	11.25	12.18	12.30	39.8	36.2	33.8

Sheffield Smoothness / IGT pick (cm)

distance	Sheffield 1	Sheffield 2	Sheffield 3	IGT pick 1	IGT pick 2	IGT pick 3
50	131	123	119	72.0	74.6	81.5
60	133	125	125	70.0	71.2	68.8
70	115	120	117	53.6	63.7	61.9
80	139	122	122	58.5	67.4	78.8
90	126	123	117	65.1	81.3	70.7
100	149	135	126	71.3	80.0	84.7
110	146	133	138	73.1	68.3	72.4
120	145	129	117	77.2	71.9	79.3
130	149	137	129	71.1	74.8	75.0

APPENDIX E
TABLE IV (cont.)

distance	pressure					
	Parker Print Surf. 10 kg/m^2			Parker Print Surf. 20 kg/m^2		
	1	2	3	1	2	3
50	4.06	4.13	4.10	3.09	3.16	3.16
60	4.03	4.12	4.24	3.06	3.13	3.25
70	3.93	3.97	4.08	3.00	3.07	3.11
80	4.18	4.16	4.18	3.17	3.16	3.18
90	4.03	3.94	4.04	3.10	3.02	3.10
100	4.24	4.18	4.11	3.24	3.19	3.13
110	4.18	4.10	4.11	3.20	3.11	3.09
120	4.18	4.05	4.02	3.19	3.08	3.05
130	4.14	3.99	4.03	3.17	3.07	3.10

APPENDIX F

Graphs of Data

Figure 10

Brightness vs. Angle

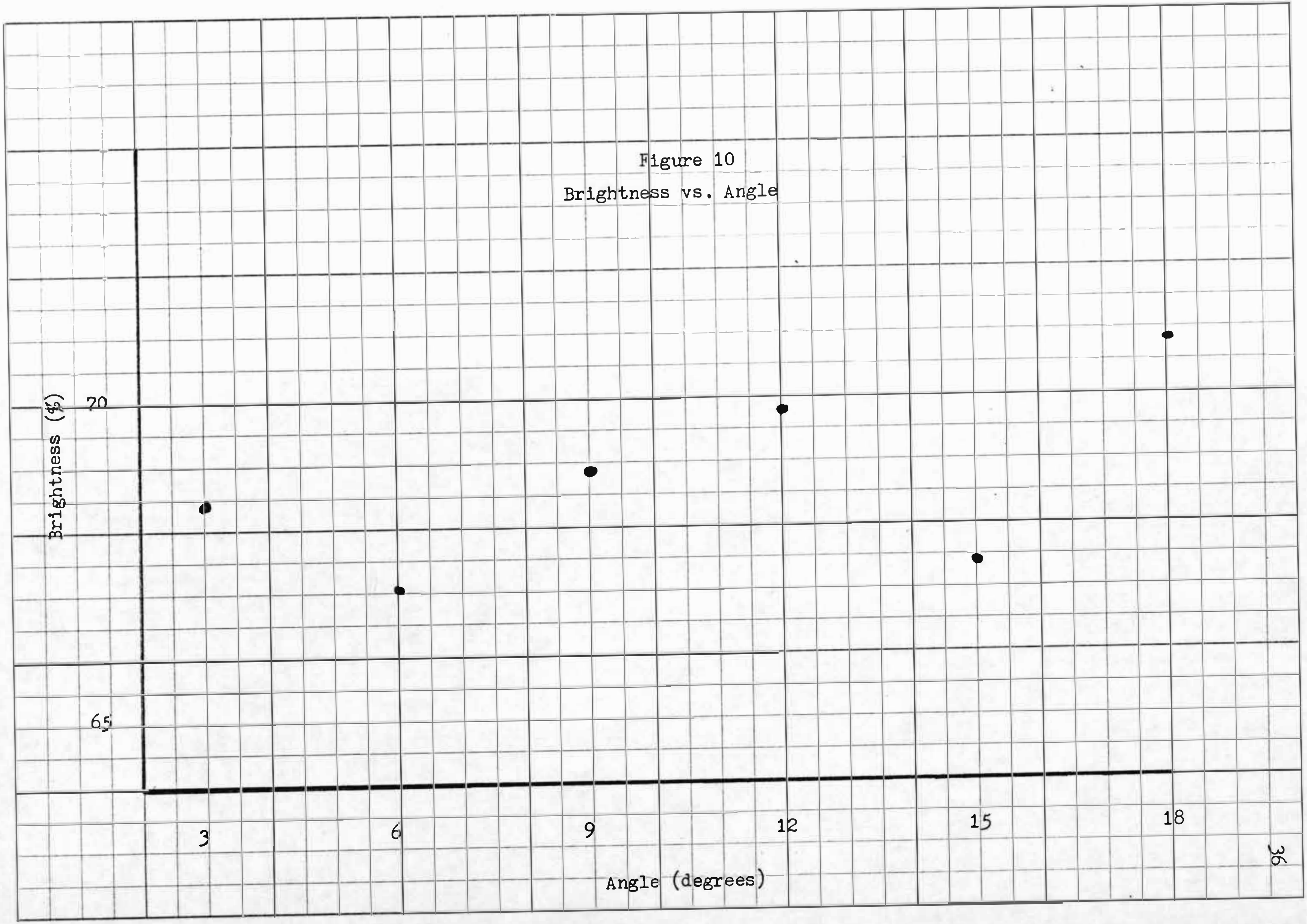

36

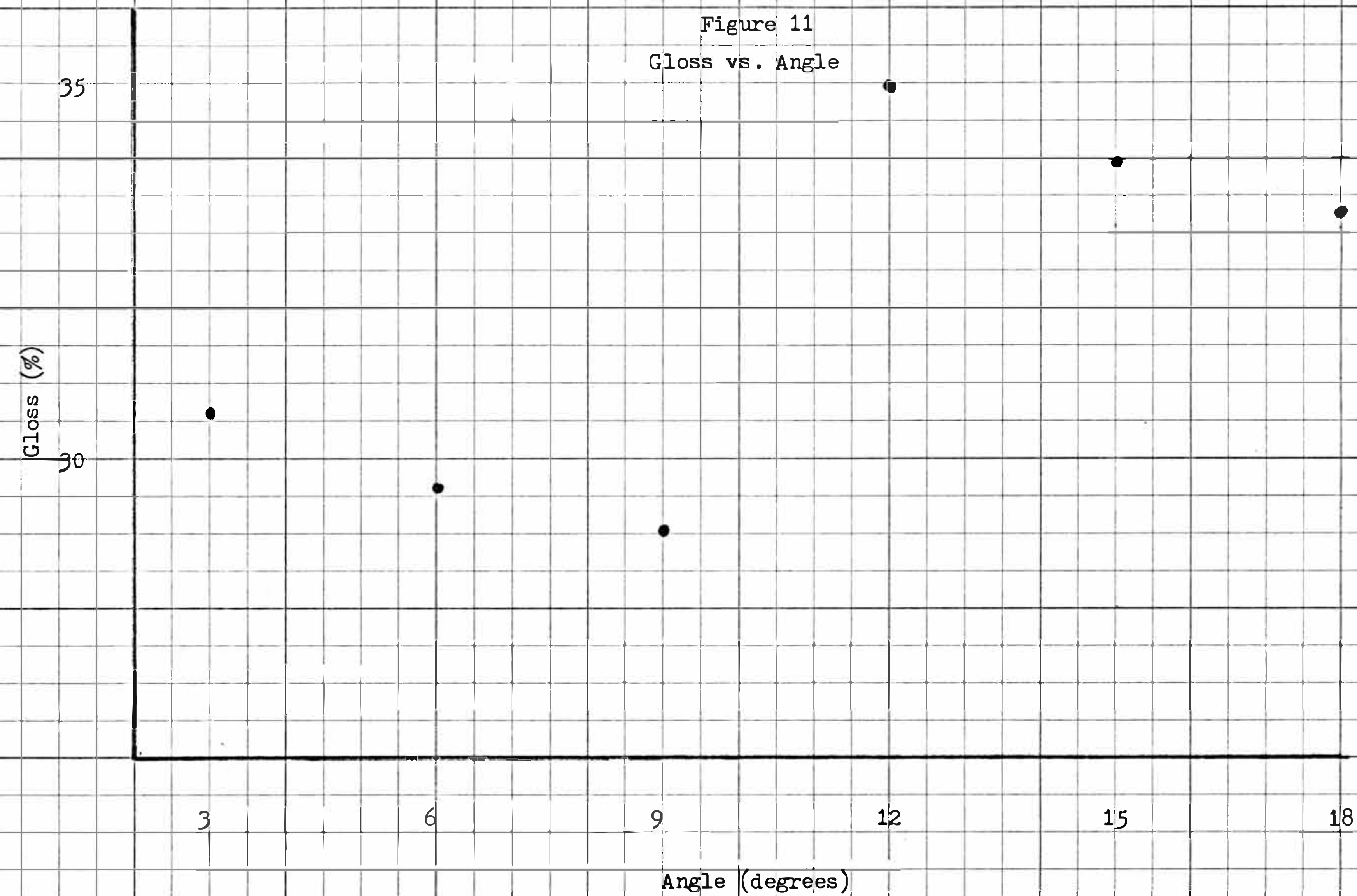
Figure 11
Gloss vs. Angle
35
30
Gloss (%)
3
6
9
12
15
18
Angle (degrees)

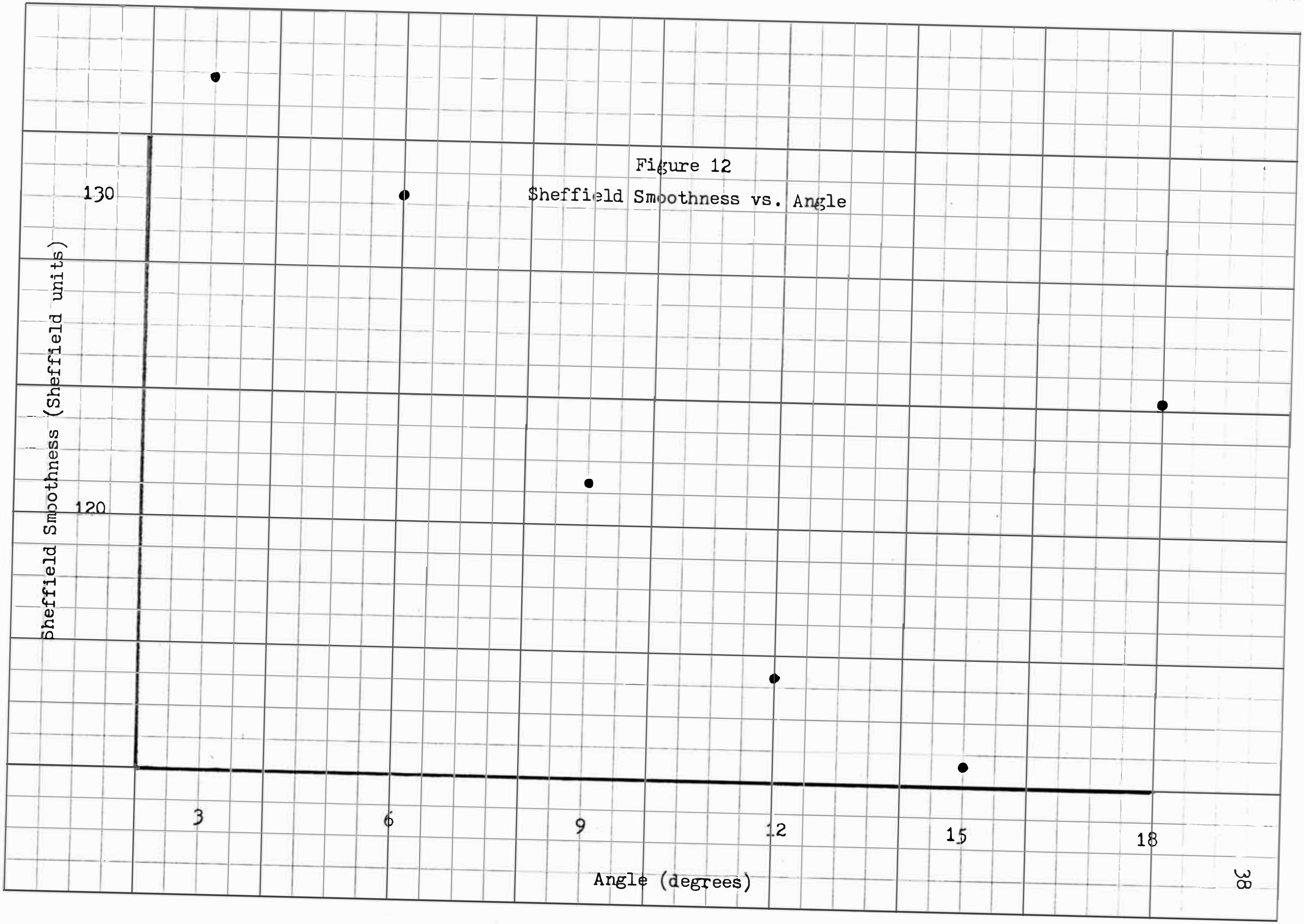

Figure 12

Sheffield Smoothness vs. Angle

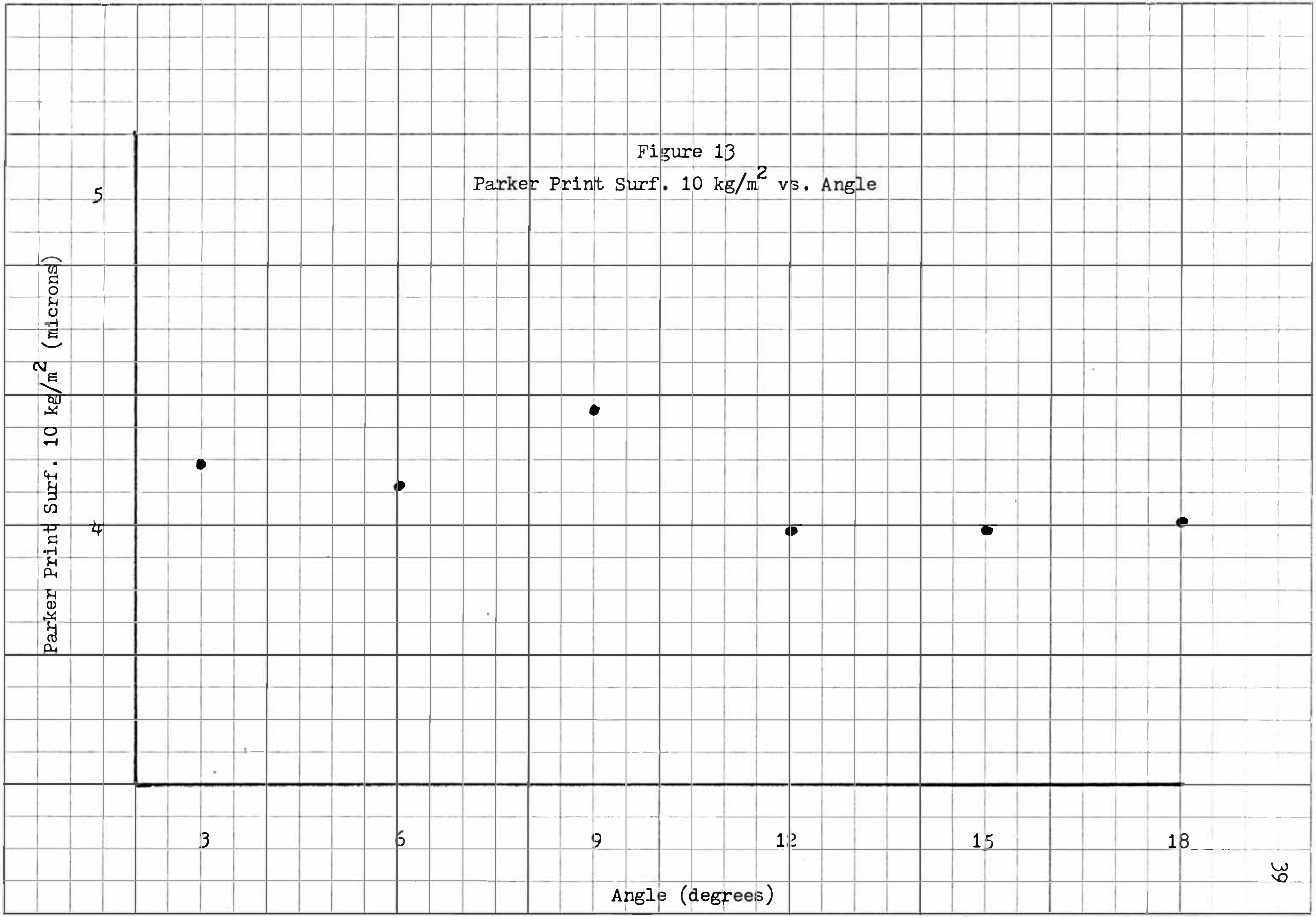

Figure 13
Parker Print Surf. 10 kg/m^2 vs. Angle

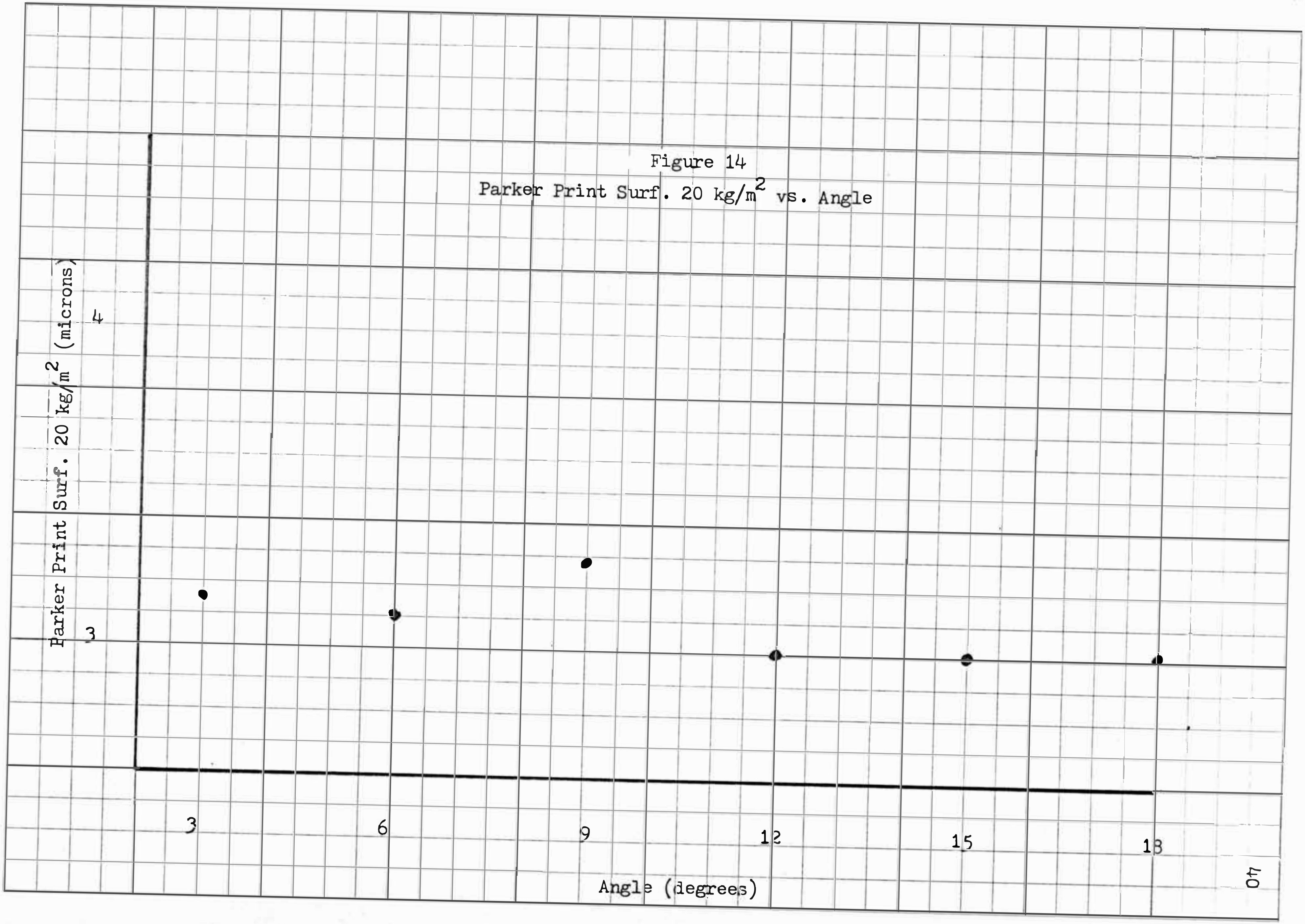

Figure 14

Parker Print Surf. 20 kg/m^2 vs. Angle

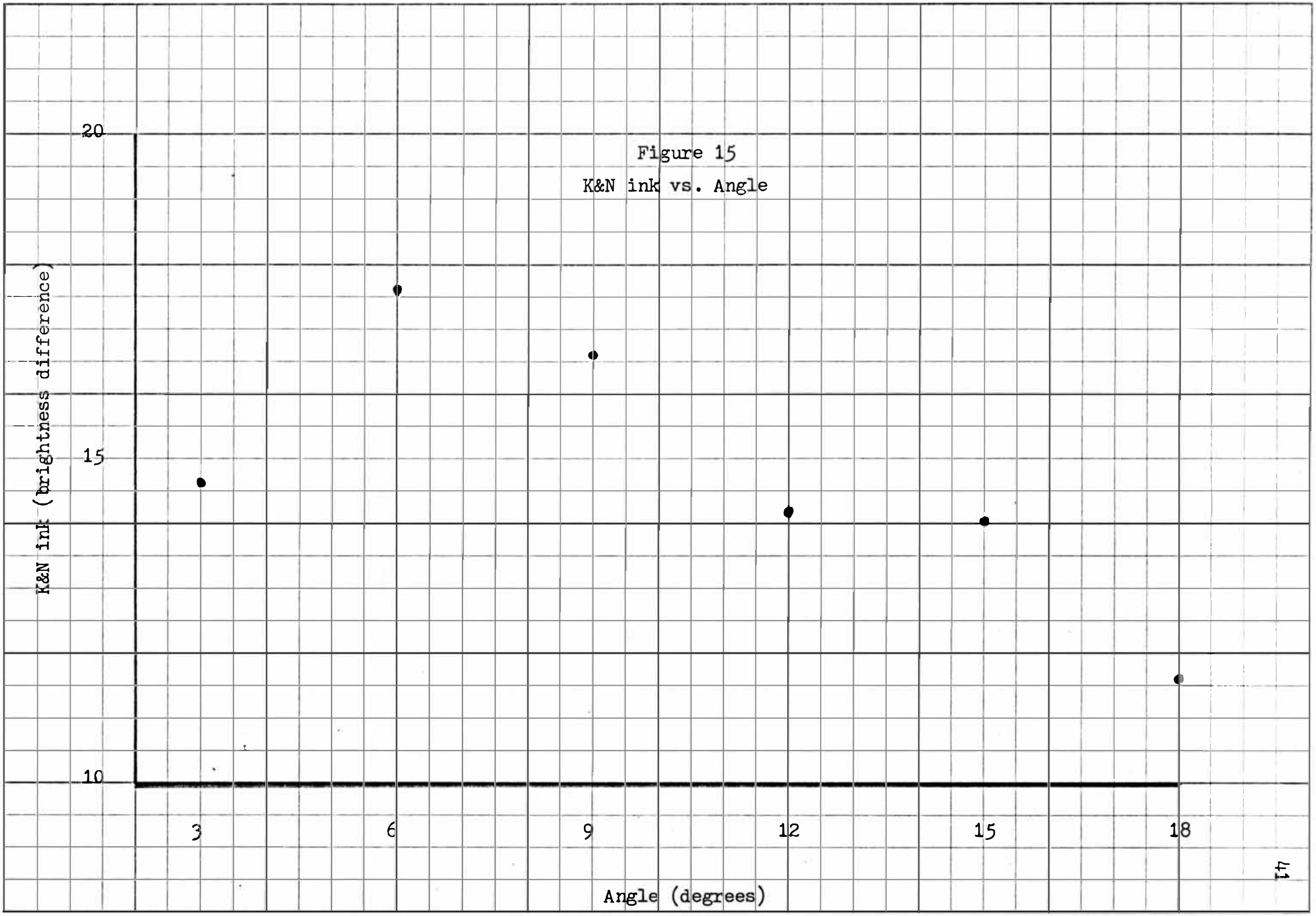

Figure 15
K&N ink vs. Angle

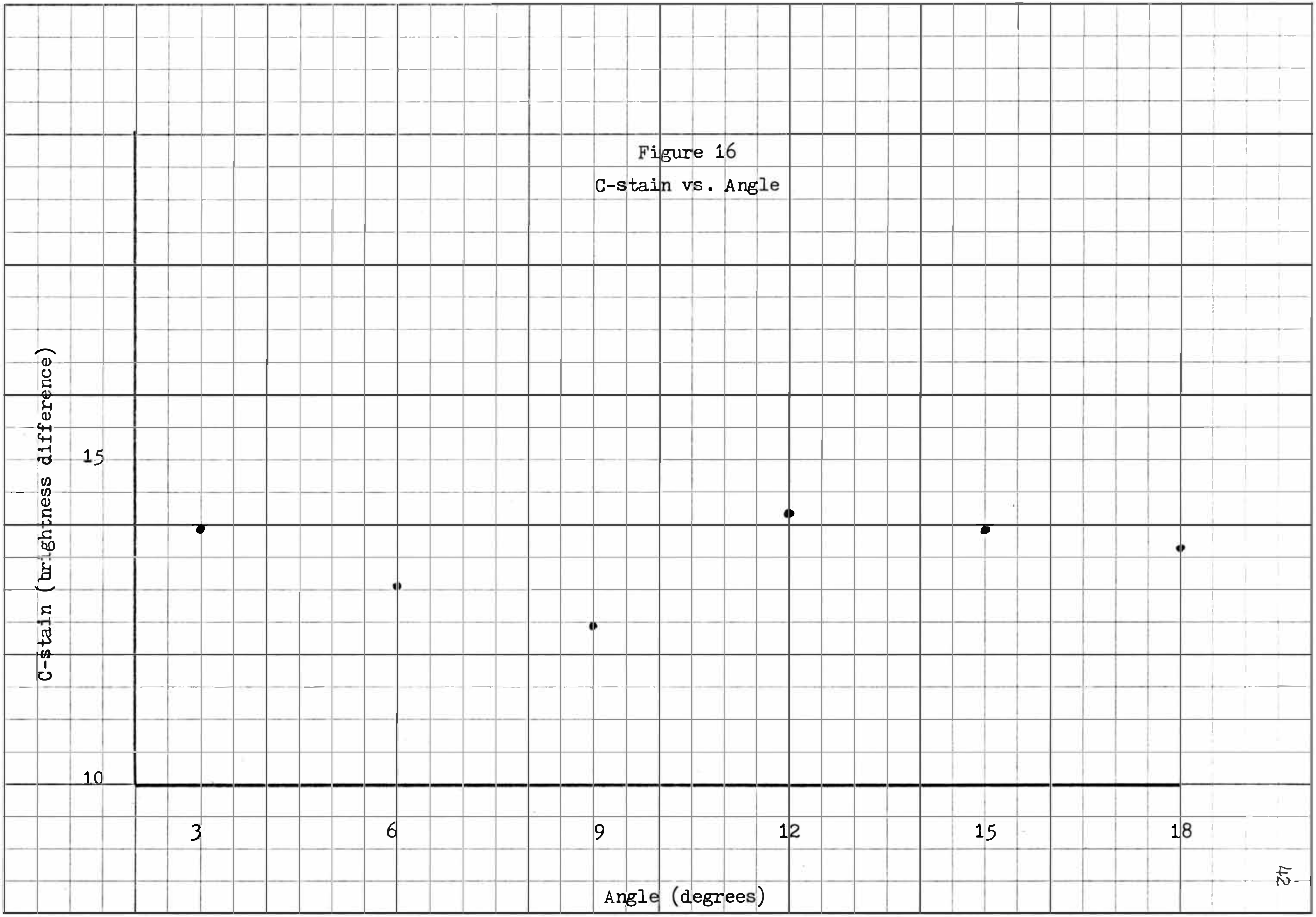
Figure 16
C-stain vs. Angle
C-stain (brightness difference)
15
10
3
6
9
12
15
18
Angle (degrees)

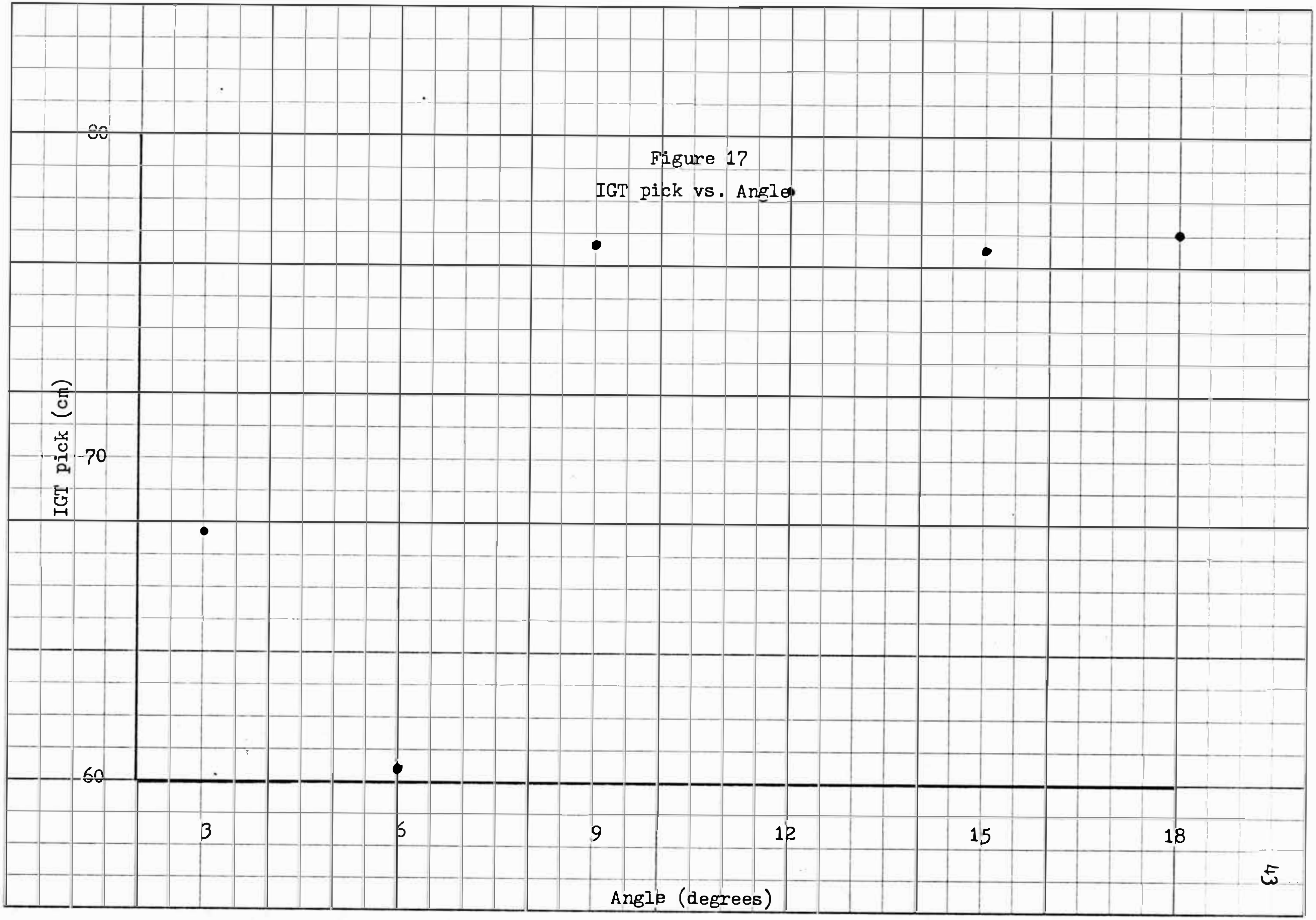
Figure 17
IGT pick vs. Angle
IGT pick (cm)
80
70
60
3
6
9
12
15
18
Angle (degrees)

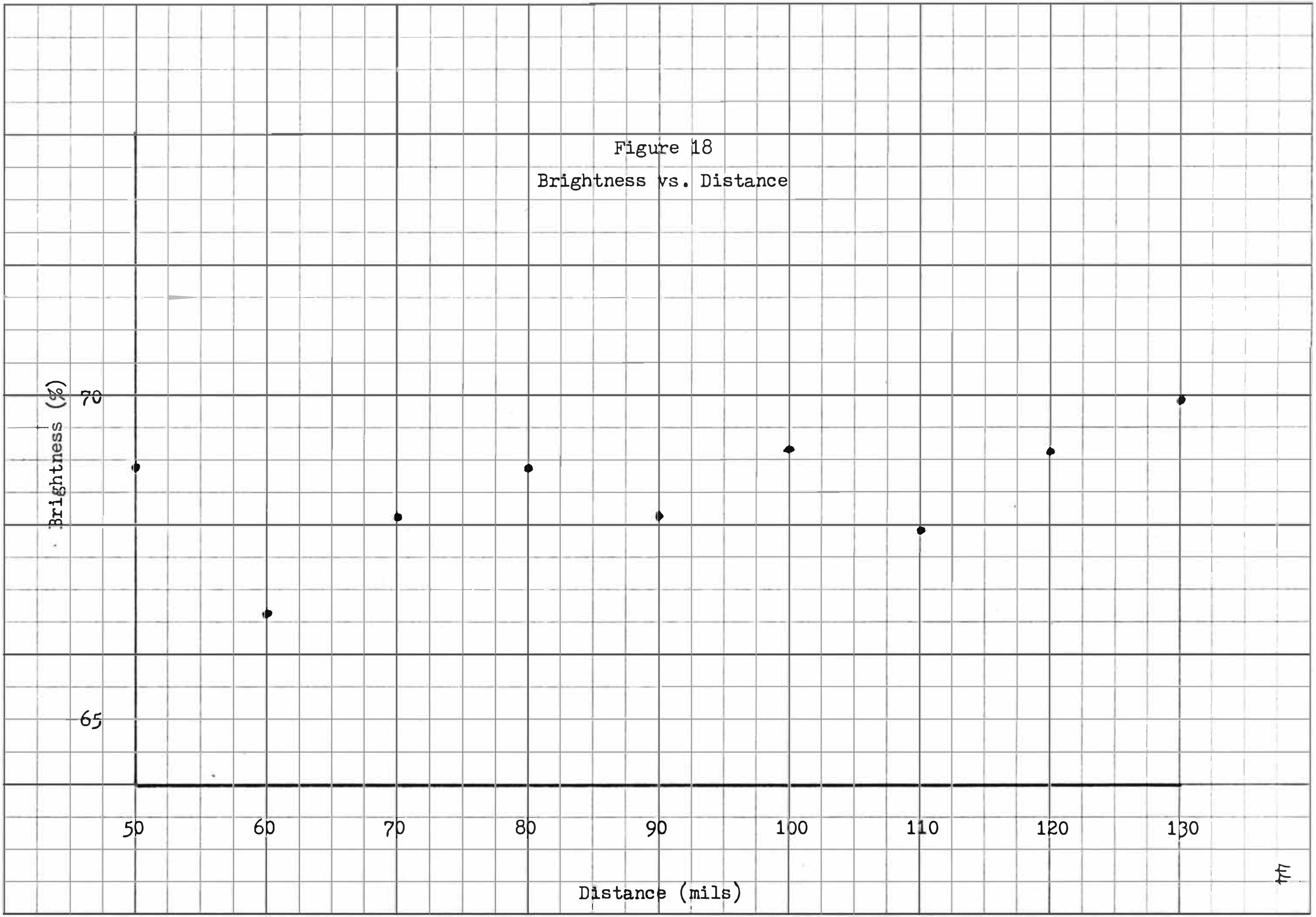
Figure 18
Brightness vs. Distance
Brightness (%)
70
65
50
60
70
80
90
100
110
120
130
Distance (mils)

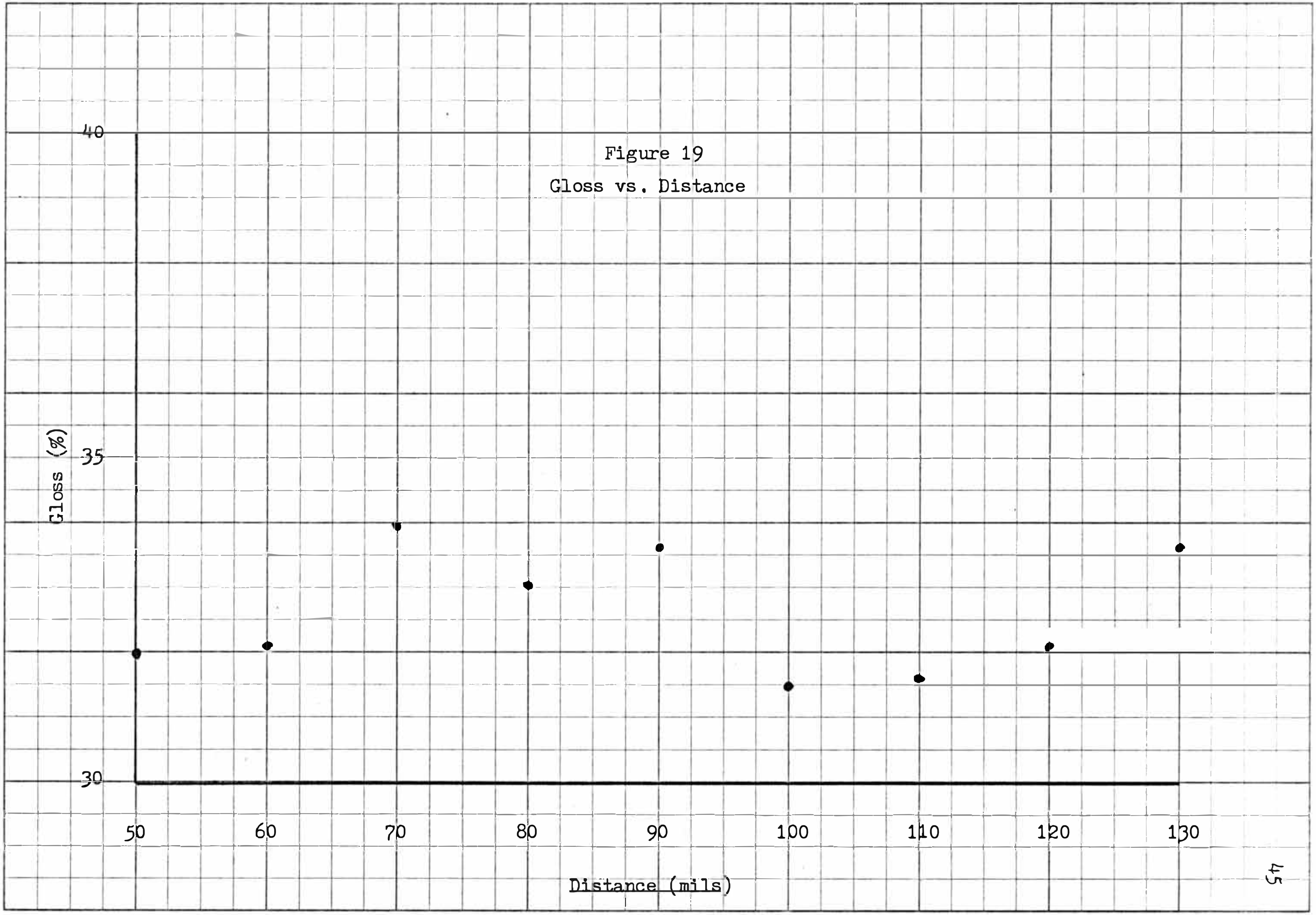
Figure 19
Gloss vs. Distance
Gloss (%)
40
35
30
50
60
70
80
90
100
110
120
130
Distance (mils)

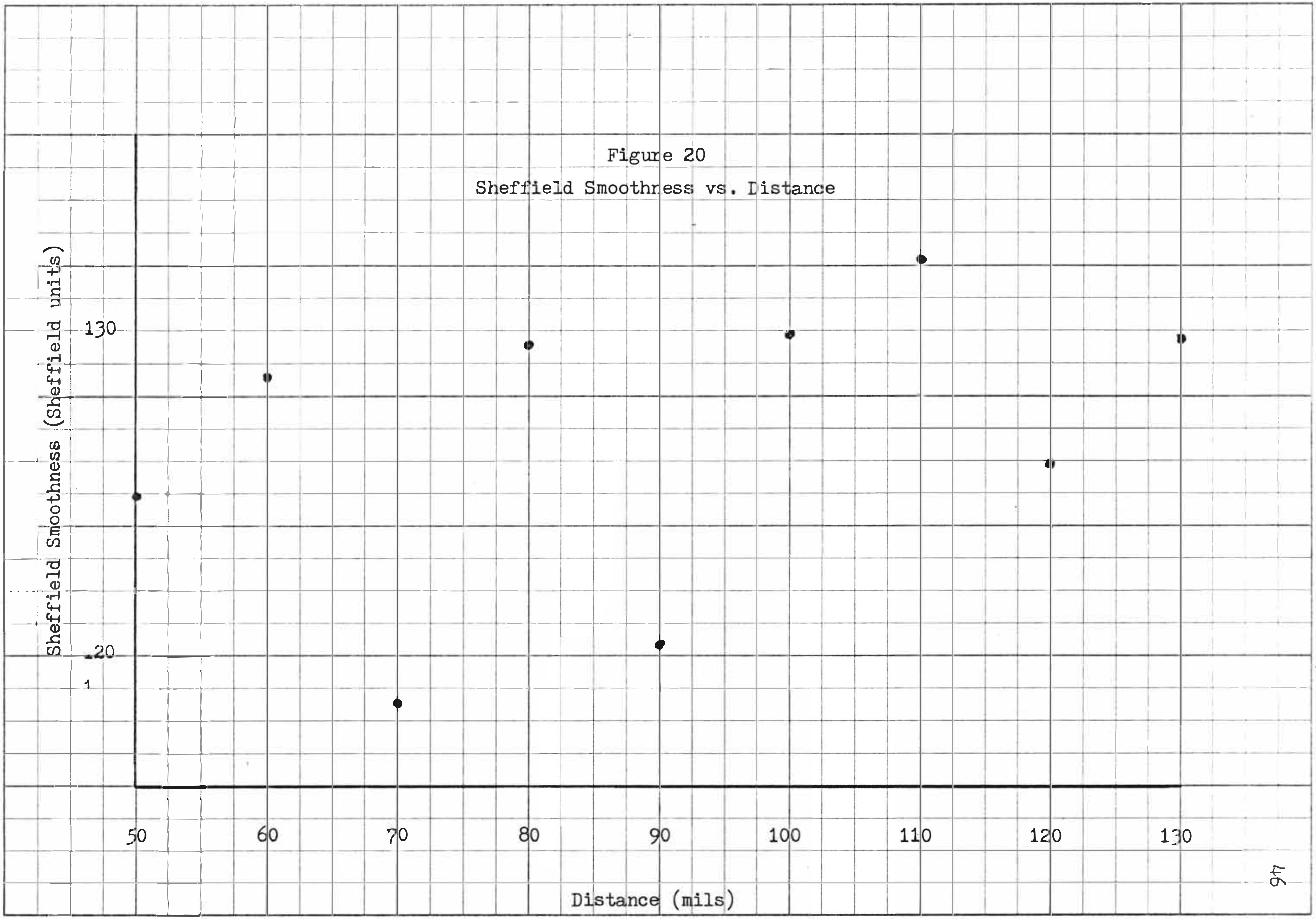

Figure 20

Sheffield Smoothness vs. Distance

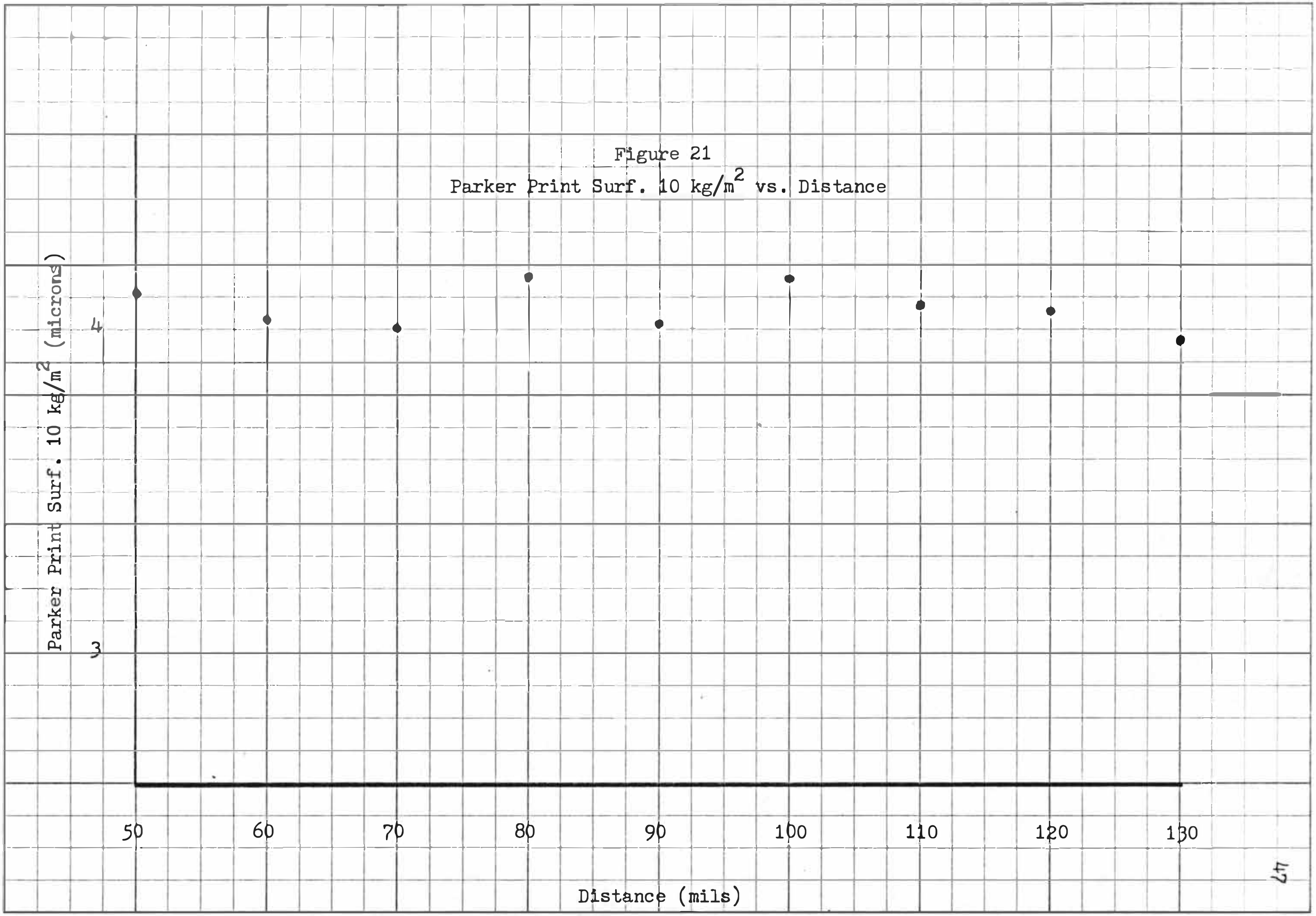

Figure 21

Parker Print Surf. 10 kg/m^2 vs. Distance

Figure 22

Parker Print Surf. 20 kg/m^2 vs. Distance

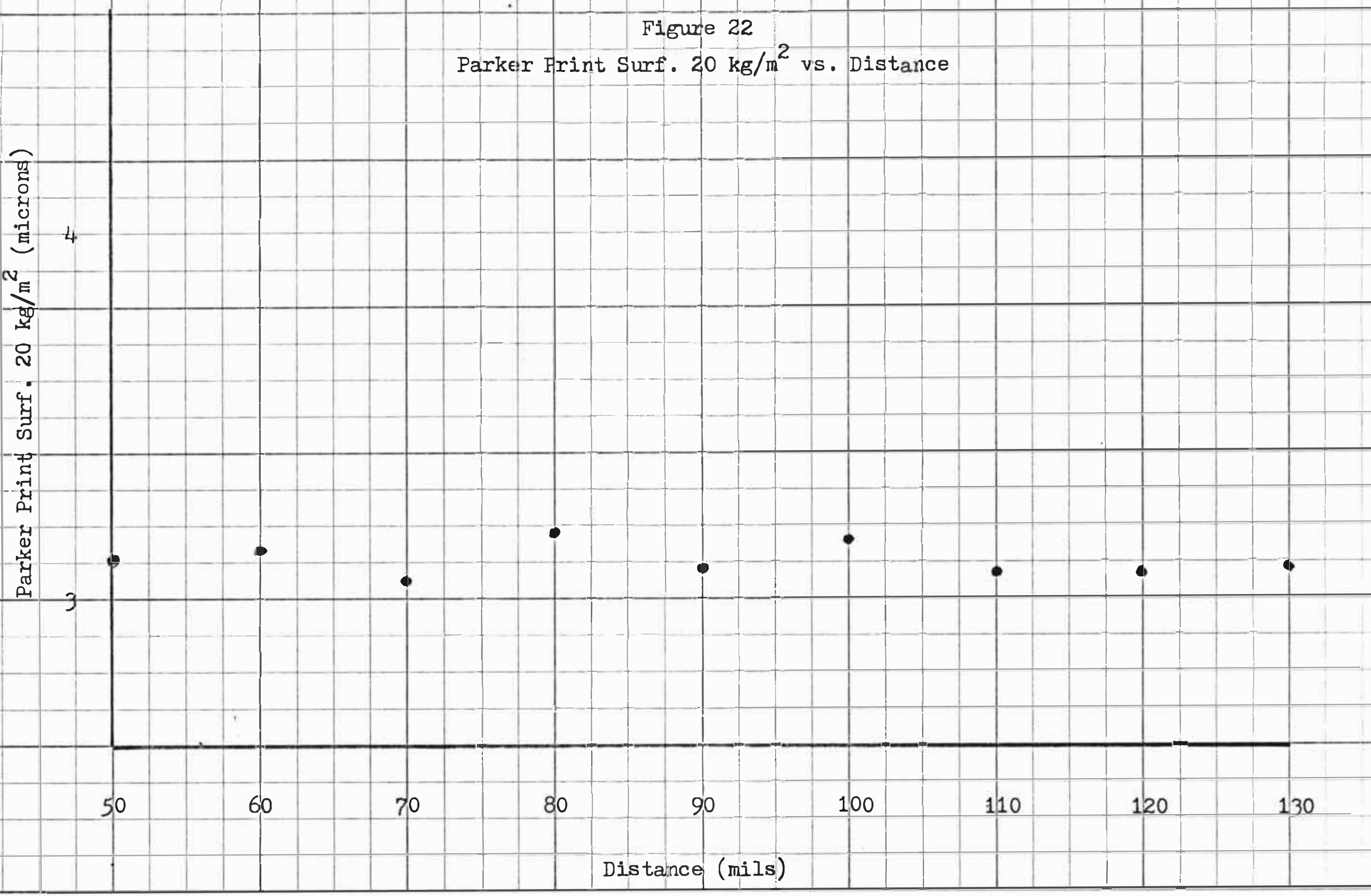

Figure 23

K&N ink vs. Distance

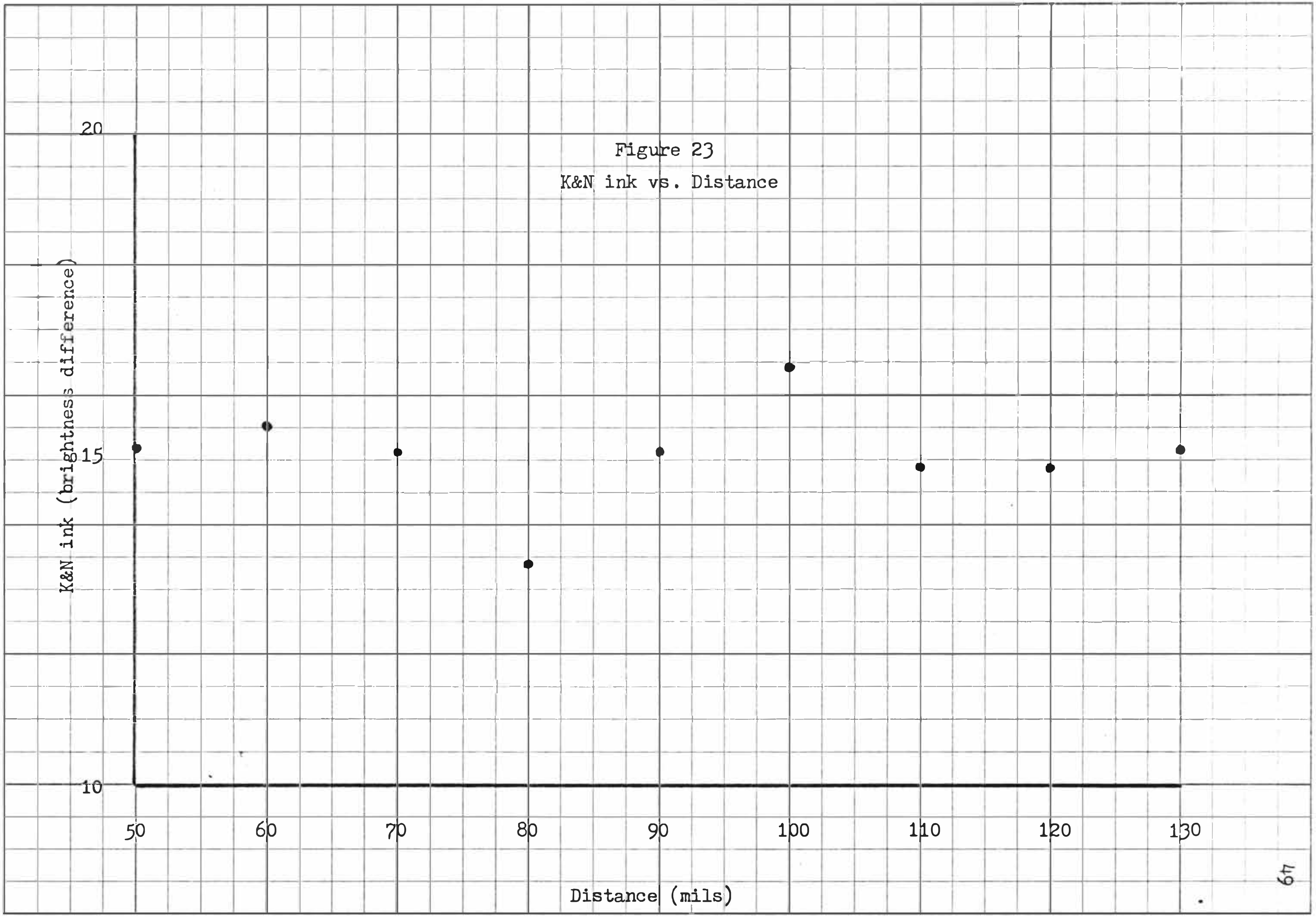

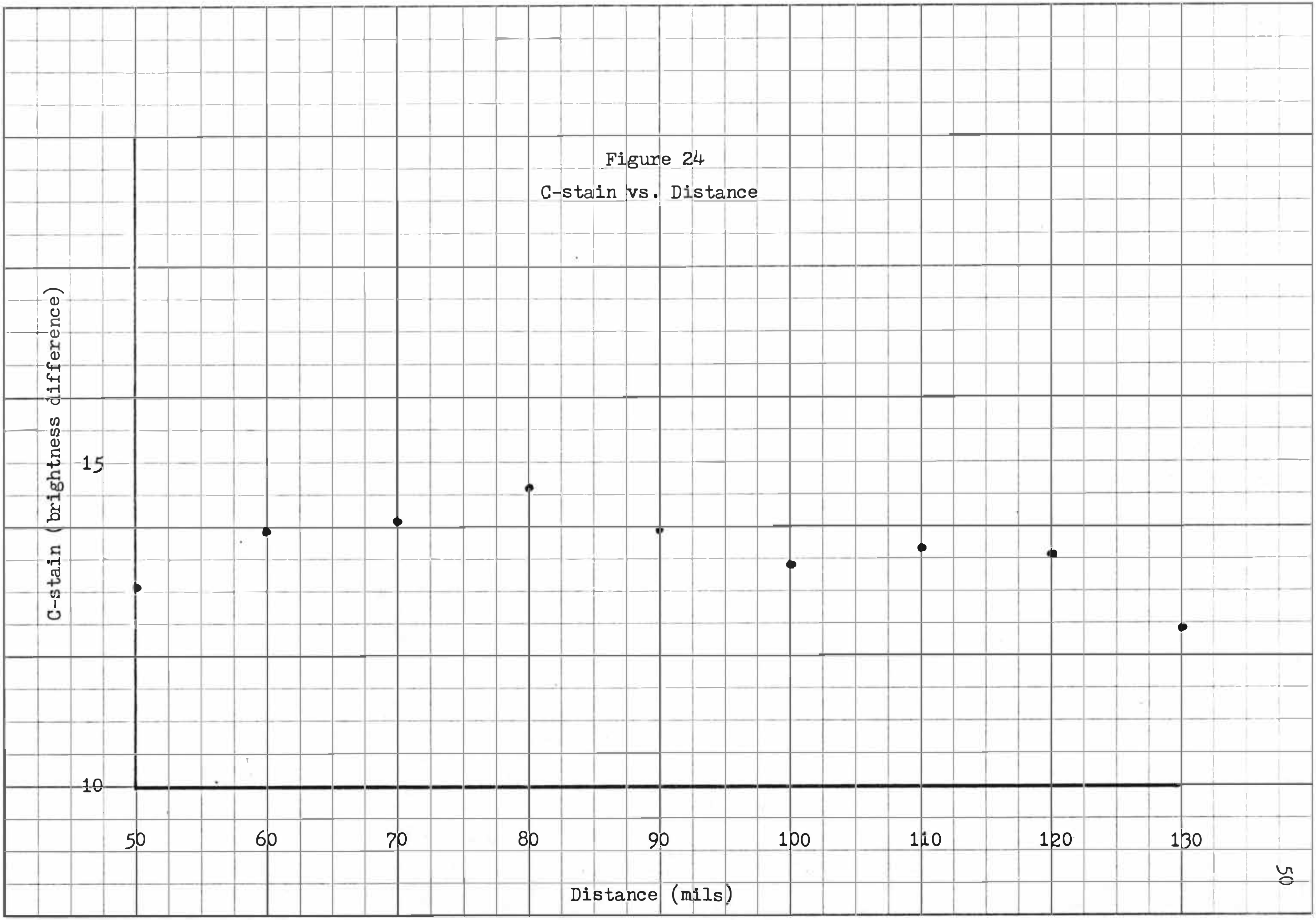

Figure 24
C-stain vs. Distance
C-stain (brightness difference)
15
10
50
60
70
80
90
100
110
120
130
Distance (mils)

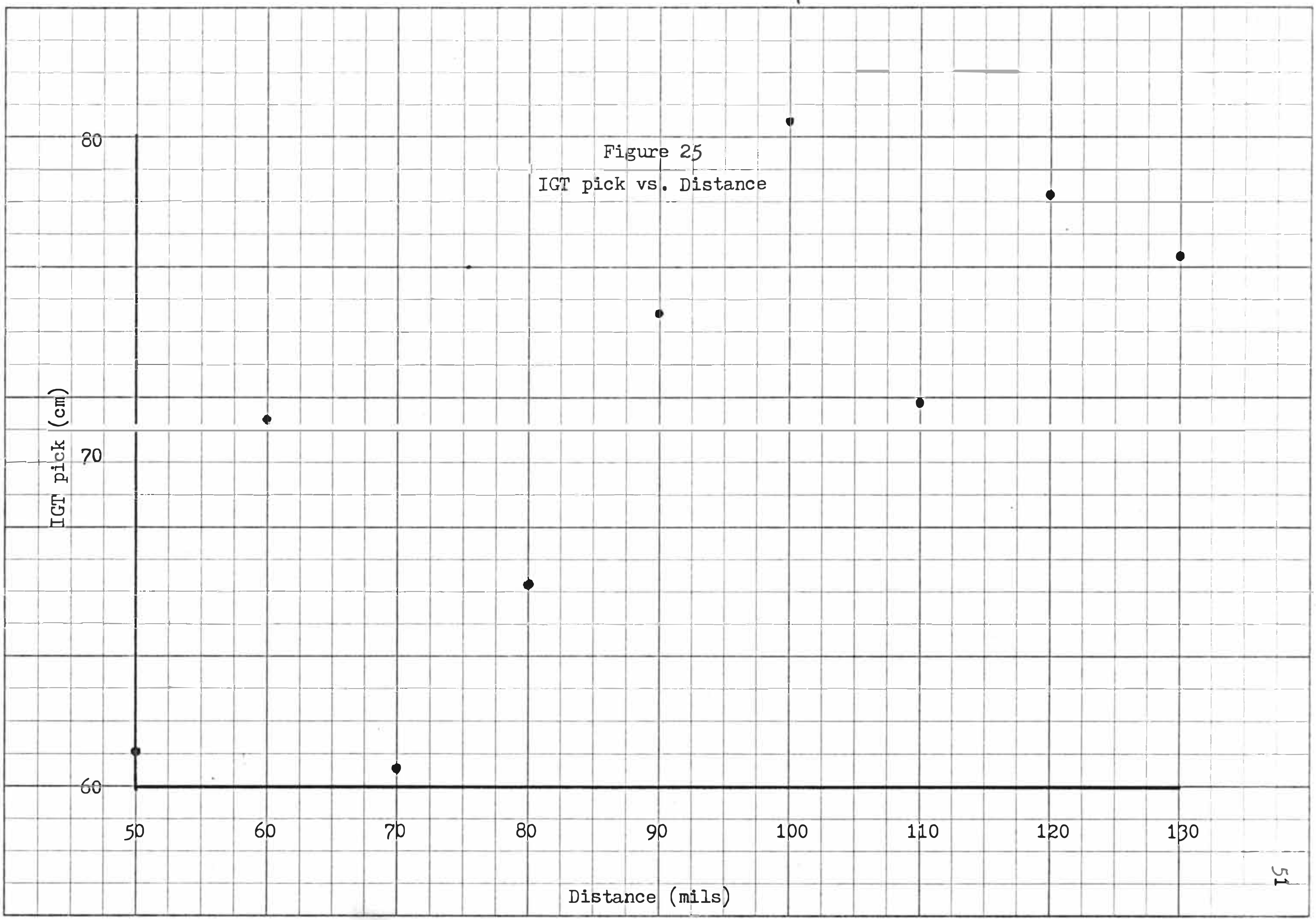
Figure 25
IGT pick vs. Distance
80
70
60
IGT pick (cm)
50
60
70
80
90
100
110
120
130
Distance (mils)